Exploring the potential of $\Delta^{17}O$ in CO_2 for determining mesophyll conductance

Adnew, Getachew Agmuas; Pons, Thijs L.; Koren, Gerbrand; Peters, Wouter; Röckmann, Thomas

Published in:
Plant Physiology

DOI:
10.1093/plphys/kiad173

https://doi.org/10.1093/plphys/kiad173 PLANT PHYSIOLOGY 2023: 192: 1234–1253

Plant Physiology®

Research Article

Exploring the potential of $\Delta^{17}O$ in CO_2 for determining mesophyll conductance

Getachew Agmuas Adnew, (ጌታቸው አግሟስ አድነው)[1,*] Thijs L. Pons,[2] Gerbrand Koren,[3] Wouter Peters[4,5] and Thomas Röckmann[1]

1 Institute for Marine and Atmospheric research Utrecht (IMAU), Utrecht University, Princetonplein 5, 3584 CC Utrecht, The Netherlands
2 Institute of Environmental Biology, Utrecht University, Padualaan 8, 3584 CH Utrecht, The Netherlands
3 Copernicus Institute of Sustainable Development, Utrecht University, Princetonlaan 8a, 3584 CB Utrecht, The Netherlands
4 Department of Meteorology and Air Quality, Wageningen University, Droevendaalsesteeg 36708PB Wageningen, The Netherlands
5 Centre for Isotope Research, University of Groningen, Nijenborgh 69747 AG Groningen, The Netherlands

*Author for correspondence: g.a.adnew@uu.nl
The author responsible for distribution of materials integral to the findings presented in this article in accordance with the policy described in the Instructions for Authors (https://academic.oup.com/plphys/pages/General-Instructions) is Getachew Agmuas Adnew.

Abstract

Mesophyll conductance to CO_2 from the intercellular air space to the CO_2–H_2O exchange site has been estimated using $\delta^{18}O$ measurements (g_{m18}). However, the g_{m18} estimates are affected by the uncertainties in the $\delta^{18}O$ of leaf water where the CO_2–H_2O exchange takes place and the degree of equilibration between CO_2 and H_2O. We show that measurements of $\Delta^{17}O$ (i.e. $\Delta^{17}O = \delta^{17}O - 0.528 \times \delta^{18}O$) can provide independent constraints on g_m ($g_{m\Delta17}$) and that these g_m estimates are less affected by fractionation processes during gas exchange. The g_m calculations are applied to combined measurements of $\delta^{18}O$ and $\Delta^{17}O$, and gas exchange in two C_3 species, sunflower (*Helianthus annuus* L. cv. 'sunny') and ivy (*Hedera hibernica* L.), and the C_4 species maize (*Zea mays*). The g_{m18} and $g_{m\Delta17}$ estimates agree within the combined errors (*P*-value, 0.876). Both approaches are associated with large errors when the isotopic composition in the intercellular air space becomes close to the CO_2–H_2O exchange site. Although variations in $\Delta^{17}O$ are low, it can be measured with much higher precision compared with $\delta^{18}O$. Measuring $g_{m\Delta17}$ has a few advantages compared with g_{m18}: (i) it is less sensitive to uncertainty in the isotopic composition of leaf water at the isotope exchange site and (ii) the relative change in the g_m due to an assumed error in the equilibration fraction θ_{eq} is lower for $g_{m\Delta17}$ compared with g_{m18}. Thus, using $\Delta^{17}O$ can complement and improve the g_m estimates in settings where the $\delta^{18}O$ of leaf water varies strongly, affecting the $\delta^{18}O$ (CO_2) difference between the intercellular air space and the CO_2–H_2O exchange site.

Introduction

During photosynthesis, CO_2 diffuses from the air surrounding the leaf through the leaf boundary layer and stomata to the intercellular air space and from there to the carboxylation site. The conductance from the intercellular air space to the carboxylation site is called mesophyll conductance. For C_3 plants, this transport path crosses different media, gas phase (intercellular air space), liquid phase (cell wall, cytosol, and stroma), and lipid–protein (plasmalemma and chloroplast envelope) (Farquhar et al. 1982; Gillon and Yakir 2000a; Evans et al. 2009). For C_4 plants, the carbon fixation step occurs in the mesophyll after conversion of CO_2 to bicarbonate (von Caemmerer et al. 2014).

Estimating mesophyll conductance (g_m) and understanding its variability in response to environmental change are

Received August 23, 2022. Accepted March 02, 2023. Advance access publication March 21, 2023

essential to improve the scientific understanding of water use efficiency (Flexas et al. 2013; Peters et al. 2018), plant–atmosphere CO_2 exchange, and gross primary productivity (GPP) of terrestrial plants (Knauer et al. 2019; Koren et al. 2019) across a range of spatial and temporal scales. g_m cannot be measured directly and its indirect determination is challenging (Warren 2006; Pons et al. 2009). Several techniques are used to estimate g_m indirectly, including the variable *J* method (Fabre et al. 2007; Flexas et al. 2007), the leaf anatomical method (Tomás et al. 2013), the curve-fitting method (Ubierna et al. 2017), the ^{13}C photosynthetic discrimination method (Evans et al. 1986), and the ^{18}O photosynthetic discrimination method (Gillon and Yakir 2000a; Barbour et al. 2016; Adnew et al. 2021). Details on these g_m measurement techniques can be found in Pons et al. (2009) and Cousins et al. (2020).

Among the isotope discrimination techniques, ^{13}C photosynthetic discrimination can only be applied to estimate mesophyll conductance (g_{m13}) of C_3 plants, whereas ^{18}O photosynthetic discrimination is suitable to measure the mesophyll conductance (g_{m18}) for both C_3 and C_4 plants. It is important to note that g_{m13} and g_{m18} in C_3 plants are not the same because the carbon and oxygen isotope signals do not represent the same diffusional pathways and process (Tholen et al. 2012). The fractionation against ^{13}C occurs primarily during carboxylation by Rubisco in the chloroplast. In C_3 plants, g_{m13} is therefore the conductance from the intercellular air space to the site of carboxylation (Cousins et al. 2020). In contrast, there is no or little enzymatic fractionation associated with assimilation of $^{12}C^{18}O^{16}O$ (and $^{12}C^{17}O^{16}O$), but the oxygen isotope effect during photosynthesis is caused by oxygen isotope exchange between CO_2 and leaf water (Farquhar and Lloyd 1993). The isotope exchange between CO_2 and H_2O involves interconversion with bicarbonate and is catalyzed by carbonic anhydrase (CA) (Gillon and Yakir 2001). In C_3 plants, CA is found in the chloroplast, cytosol, mitochondria, and the plasma membrane (Badger and Price 1994; Fabre et al. 2007; DiMario et al. 2016), and the CO_2–H_2O exchange can occur anywhere between the plasma membrane and chloroplast (Ogée et al. 2018). For C_4 plants, CA is mainly found in the cytosol where CO_2–H_2O exchange occurs (Badger and Price 1994; Ogée et al. 2018). g_{m18} is thus the conductance of CO_2 as it diffuses from the intercellular air space to the site of CO_2–H_2O exchange for both C_3 and C_4 plants (Gillon and Yakir 2000a, 2000b; Barbour et al. 2016).

The oxygen isotope composition of leaf water at the point where the CO_2–H_2O exchange takes place is a key source of uncertainty in the estimation of g_m using oxygen isotopes because a considerable and strongly variable oxygen isotope variation can develop within the leaf due to the discrimination associated with evaporation, transport, and diffusion of H_2O (Gan et al. 2002; Cousins et al. 2006; Song et al. 2015; Cernusak et al. 2016). Furthermore, $\delta^{18}O$ increases sharply along the leaf blade, especially for C_4 grasses (narrower interveinal distances) (Helliker and Ehleringer 2000; Gan et al. 2003; Landais et al. 2006). Recently, Holloway-Phillips et al. (2019) explored the use of ^{18}O-enriched CO_2 and ^{18}O-enriched water vapor to improve g_{m18} estimates and provided guidelines to minimize the sensitivity of g_{m18} estimates to measurement errors. Importantly, g_{m18} estimates are more precise when the difference in $\delta^{18}O$ of the CO_2 between the intercellular air space and CO_2–H_2O exchange site is large (Holloway-Phillips et al. 2019). A larger $\delta^{18}O$ difference can be achieved by manipulating the $\delta^{18}O$ of the CO_2 or the water vapor entering the leaf cuvette used for the measurements, and/or $\delta^{18}O$ value of the irrigation water.

In this study, we investigated the application of $\Delta^{17}O$ (the deviation from a reference relationship between $^{17}O/^{16}O$ and $^{18}O/^{16}O$, see section Theory) to estimate the mesophyll conductance. Figure 1 illustrates how $\Delta^{17}O$ measurements can be utilized to estimate g_m which, in principle, is equivalent to the one using $\delta^{18}O$. Whereas $\delta^{17}O$ and $\delta^{18}O$ vary strongly depending on time of day, environmental conditions, and geographical location (Gat 1996; Angert et al. 2003; Barkan and Luz 2007; Landais et al. 2008; Luz and Barkan 2010; Uemura et al. 2010; Risi et al. 2013; Aron et al. 2021), $\Delta^{17}O$ is less affected (Landais et al. 2006; Song et al. 2015; Cernusak et al. 2016) since the three-isotope slopes (the relationship between $^{17}O/^{16}O$ and $^{18}O/^{16}O$) of the contributing processes are rather similar. In particular, the large variations in the isotopic composition of meteoric water do not affect $\Delta^{17}O$ when the reference slope of meteoric water $\lambda = 0.528$ is chosen, and the effect of water evaporation from the leaf is much smaller for $\Delta^{17}O$ compared with $\delta^{18}O$ (or $\delta^{17}O$). Therefore, we hypothesized that the uncertainty in the isotopic composition of H_2O at the CO_2–H_2O exchange site and the assigned degree of equilibration (θ_{eq}) between H_2O and CO_2 would introduce smaller errors to mesophyll conductance estimates based on $\Delta^{17}O$ measurements compared with estimates using $\delta^{18}O$ measurements.

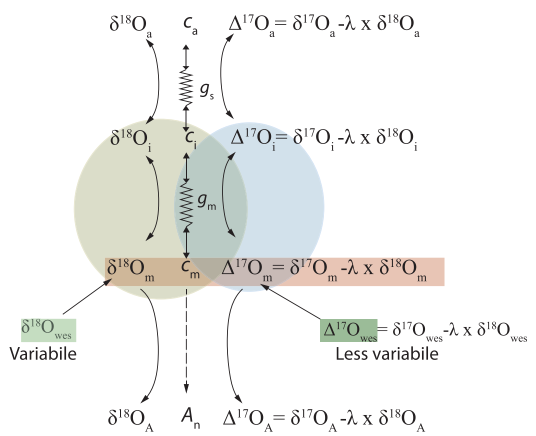

Figure 1. Schematic showing the parameters used to calculate mesophyll conductance using $\delta^{18}O$ (g_{m18}) and $\Delta^{17}O$ ($g_{m\Delta17}$). A_n is net assimilation. The subscripts *a*, *i*, *m*, *wes*, and *A* stand for atmosphere, intercellular air space, mesophyll, water at the evaporation site, and assimilation, respectively.

We performed gas exchange measurements for the estimation of g_{m18} and $g_{m\Delta17}$ with two C_3 and one C_4 species at two photon flux densities (PFD), generating a wide variation in c_m/c_a ratios (c_m and c_a are the mole fraction of CO_2 at the CO_2–H_2O exchange site and, in the air, surrounding the leaf, respectively). The data were previously used to estimate the effect of photosynthetic gas exchange on the $\Delta^{17}O$ of atmospheric CO_2 (Adnew et al. 2020). To quantify the sensitivity of the g_{m18} and $g_{m\Delta17}$ estimates to various parameters, we used Monte Carlo simulations and a leaf cuvette model (Adnew et al. 2020; Koren et al. 2020). The leaf cuvette model and analytical equations for gas exchange (von Caemmerer and Farquhar 1981; Farquhar and Cernusak 2012) were used to quantify the uncertainty due to potential errors in the assumption of the oxygen isotope composition of leaf water at the CO_2–H_2O exchange site.

Theory

Oxygen isotopes

Oxygen has two heavy isotopes ^{17}O and ^{18}O, with respective natural abundances of approximately 0.038% and 0.2%. Since most isotope fractionation processes depend on mass, the variations in $\delta^{17}O$ and $\delta^{18}O$ are closely related as follows (Matsuhisa et al. 1978; Young et al. 2002):

$$\frac{^{17}R_{\text{sample}}}{^{17}R_{\text{reference}}} = \left(\frac{^{18}R_{\text{sample}}}{^{18}R_{\text{reference}}}\right)^{\lambda} \quad (1)$$

where $^{17}R = {}^{17}O/{}^{16}O$ and $^{18}R = {}^{18}O/{}^{16}O$ and λ is referred to as the three-isotope exponent. Equation (1) can be written in δ notation as follows:

$$(\delta^{17}O + 1) = (\delta^{18}O + 1)^{\lambda} \text{ or} \quad (2)$$

$$\ln(\delta^{17}O + 1) = \lambda \times \ln(\delta^{18}O + 1) \quad (3)$$

where $\delta^{17}O = ({}^{17}R_{\text{sample}} - {}^{17}R_{\text{reference}})/{}^{17}R_{\text{reference}}$ and $\delta^{18}O = ({}^{18}R_{\text{sample}} - {}^{18}R_{\text{reference}})/{}^{18}R_{\text{reference}}$. Theoretical considerations suggest that λ varies from 0.5000 to 0.5305 for different mass-dependent isotope fractionation processes, but recent studies have reported λ values even outside this range (Hayles et al. 2017; Adnew et al. 2022; Hayles and Killingsworth 2022). Deviations from Equation (3) are quantified as $\Delta^{17}O$, and in this study, we used the linearized definition for $\Delta^{17}O$.

$$\Delta^{17}O = \delta^{17}O - \lambda \times \delta^{18}O \quad (4)$$

Note that the Δ symbol is also commonly used for isotopic discrimination or enrichment in biological studies, but we use it here to quantify the relative deviations from the linearized Equation (3), as shown in Equation (4). For discrimination associated with assimilation, we use Δ_A [see Equations (12) and (14)] similar to Farquhar and Lloyd (1993) and Farquhar et al. (1993). For the different isotope signals, we use $\Delta_A^{13}C$, $\Delta_A^{18}O$, $\Delta_A^{17}O$, and $\Delta_A\Delta^{17}O$.

$\Delta^{17}O$ of CO_2 has been suggested as a tracer for constraining gross primary production (GPP), the total CO_2 uptake by the plants (Hoag et al. 2005; Thiemens et al. 2014; Hofmann et al. 2017; Liang et al. 2017; Koren et al. 2019). Whereas $\delta^{18}O$ is strongly affected by kinetic and equilibrium fractionation processes between CO_2 and substrate water and source water isotopic inhomogeneity and dynamics, $\Delta^{17}O$ variations are much smaller and are better defined (Hoag et al. 2005; Liang et al. 2017). This is because conventional biogeochemical processes that modify $\delta^{17}O$ and $\delta^{18}O$ follow a well-recognized three-isotope fractionation slope (Young et al. 2002; Barkan and Luz 2005, 2007; Hoag et al. 2005; Landais et al. 2006) (see Fig. 1). For specific process, $\Delta^{17}O$ is less sensitive to fractionations due to physicochemical processes than $\delta^{17}O$ and $\delta^{18}O$ (Cao and Liu 2011; Hofmann et al. 2012). $\Delta^{17}O$ can also generally be measured with a better external precision than $\delta^{17}O$ and $\delta^{18}O$ (Miller et al. 1999), since mass-dependent fractionations due to experimental gas handling cancel out (Thiemens 2006). However, measurements of $\Delta^{17}O$ of CO_2 are technically more challenging and therefore not widely used. Recent advances in measurement techniques such as the CO_2–O_2 exchange method (Mahata et al. 2013; Barkan et al. 2015; Adnew et al. 2019), the O-fragment method (Adnew et al. 2019), and laser spectroscopy techniques (McManus et al. 2005; Stoltmann et al. 2017; Steur et al. 2021) make it possible to measure $\Delta^{17}O$ of CO_2 with a precision better than 0.01‰.

$\Delta^{17}O$ of leaf water and CO_2 during leaf gas exchange

Figure 1 schematically shows how different processes that are involved in leaf–atmosphere exchange affect $\delta^{18}O$, $\delta^{17}O$, and $\Delta^{17}O$ of H_2O (both liquid and vapor) and CO_2 due to the different process-specific three-isotope slopes (θ) relative to a reference three-isotope slope of $\lambda = 0.528$. Note that the choice of the reference slope (λ) is arbitrary since in nature, isotopic compositions rarely reflect fractionation from a single process but instead integrate multiple fractionating processes and several θ values (Young et al. 2002; Barkan and Luz 2005, 2007; Landais et al. 2006). Here, we choose the value $\lambda = 0.528$ associated with meteoric water (Meijer and Li 1998; Luz and Barkan 2010).

Plants take up meteoric water (located on the reference line) via the roots, and there is negligible fractionation in stem water, which feeds the leaf (Cernusak et al. 2016). The preferential evaporation of $H_2^{16}O$ relative to the heavier isotopologs leads to an isotope enrichment of the leaf water that depends strongly on the opening of the stomata and the vapor pressure deficit (VPD) (Gat 1996; Farquhar et al. 2007; Gonfiantini et al. 2018). The effect on $\delta^{18}O$ therefore shows a strong temporal (diurnal) variability. The three-isotope slope for liquid–vapor equilibration is well constrained (i.e. $\theta_{H2O(v)-H2O(l)} = 0.529$), and when the water evaporates, $\delta^{17}O$ and $\delta^{18}O$ of the residual leaf water move upward on this line as shown in Fig. 2A (from points A to B, Fig. 1A) while the water

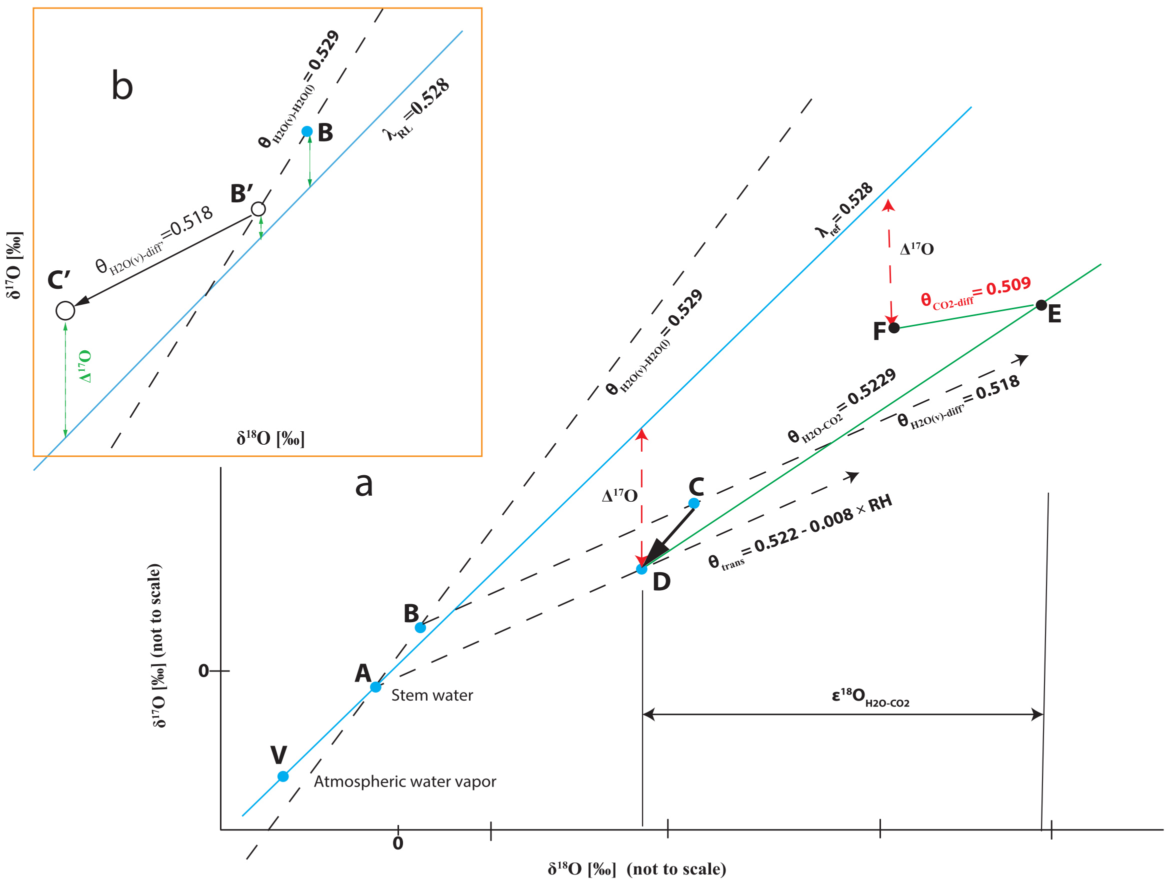

Figure 2. Oxygen isotope fractionations of $\Delta^{17}O$ of CO_2 and H_2O during photosynthetic gas exchange. **A)** A schematic for isotope fractionations that affect the $\Delta^{17}O$ of CO_2 and H_2O during leaf atmosphere gas exchange (not to scale), including interaction of leaf water with atmospheric water vapor. The triple oxygen isotope relationships for the individual isotope fractionation processes (both kinetic and equilibrium fractionations) are given as θ-values. $\theta_{trans} = 0.522 - 0.008 \times RH$ (Landais et al. 2006), $\theta_{CO2-H2O} = 0.5229$ (Barkan and Luz 2012), $\theta_{CO2-diff} = 0.509$ (Young et al. 2002), $\theta_{H2O(v)-H2O(l)} = 0.529$ (Barkan and Luz 2005), and $\theta_{H2O(v)-diff} = 0.518$ (Barkan and Luz 2007), where "*v*" and "*l*" are vapor and liquid water, respectively. The $\epsilon^{18}O$ values quantify the enrichment or depletion in the ^{18}O isotope composition due to the corresponding isotope fractionation process, and "diff" and "trans" refer to diffusion and transpiration, respectively. **A)** shows only the liquid water (leaf water) and the CO_2 that undergo exchange with leaf water and diffuse out of the leaf. **B)** The effect of evaporation of water in $\delta^{17}O$–$\delta^{18}O$ space showing the $\Delta^{17}O$ and $\delta^{18}O$ changes for equilibration between liquid and gas phase water and diffusion of water vapor. Note that **B)** does not show interaction with atmospheric water vapor. B′ and C′ are the water vapor in equilibrium with leaf water in the intercellular air space (with point B) and water vapor diffused through stomata to the atmosphere, respectively.

vapor in equilibrium with leaf water moves downward (from points B to B′, Fig. 2B) (Barkan and Luz 2005). As a result, the $\Delta^{17}O$ value of the residual liquid water will be slightly higher compared with the stem water. However, molecular diffusion of equilibrated water vapor through the stomata is associated with a θ-value of 0.518 (Barkan and Luz 2007). Molecular diffusion results in an enrichment in the $\delta^{17}O$ and $\delta^{18}O$ of leaf water (points B to C, Fig. 2A) while the diffused water vapor is depleted in $\delta^{17}O$ and $\delta^{18}O$ (B′ to C′, Fig. 1B). Since the θ-value for diffusion of water vapor is lower than the reference slope (0.518 vs 0.528), the $\Delta^{17}O$ of the diffused vapor is higher than the one of the residual leaf water (Figs. 1A and 2B) (Barkan and Luz 2007). The magnitude of the fractionation due to diffusion (points B to C) depends on the VPD: the higher the VPD, the higher the fractionation due to the molecular diffusion of water vapor through the stomata.

Via stomatal exchange, atmospheric water vapor also affects the isotopic composition of leaf water at the evaporation site (points C to D, Fig. 2A). In general, exchange and mixing between leaf water and atmospheric water vapor will result in a decrease in $\delta^{17}O$ and $\delta^{18}O$ of the leaf water. The overall 3-isotope slope between stem water and leaf water due to the abovementioned processes that affect evapotranspiration has been determined to be a function of relative humidity ($\theta_{trans} = 0.522 - 0.008 \times RH$) (Fig. 2A; Landais et al. 2006).

When CO_2 enters the plant, its oxygen isotope composition will equilibrate with leaf water at the exchange site (points D to E). The $\delta^{17}O$ and $\delta^{18}O$ value of the equilibrated

CO_2 is higher than the one of leaf water, while the $\Delta^{17}O$ value of the CO_2 will be lower than the leaf water (Brenninkmeijer et al. 1983; Barkan and Luz 2012). After isotope exchange with leaf water, part of the CO_2 diffuses back to the atmosphere with a θ-value of 0.509 (Young et al. 2002), which results in a relatively higher $\Delta^{17}O$ value and lower $\delta^{17}O$ and $\delta^{18}O$ values compared with the CO_2 in equilibrium with leaf water (points E to F, Fig. 2A). We note that the $\Delta^{17}O$ value of CO_2 diffusing out from the leaf can end up below or above the reference line depending on how negative or positive the $\Delta^{17}O$ value of the CO_2 at the CO_2–H_2O site is. Still, the variations in $\Delta^{17}O$ are much smaller than the signals in $\delta^{18}O$, as described below.

The effect of each process on the $\Delta^{17}O$ value of either H_2O or CO_2 can be quantified using the $\delta^{18}O$ fractionation of that process (ϵ_p) and the three-isotope slope of the specific process (θ_p) (Hofmann et al. 2017; Koren et al. 2019; Adnew et al. 2020), as shown in Equation (5).

$$\Delta^{17}O_P \approx (\theta_P - \lambda_{RL}) \times \varepsilon_P \quad (5)$$

For instance, when leaf water is enriched in $\delta^{18}O$ by $\epsilon^{18}O_{diff}$ due to diffusion, its $\Delta^{17}O$ value changes only by $(\theta_{diff} - \lambda_{RL}) \times \epsilon^{18}O_{diff}$. Since $\theta_{diff} - \lambda_{RL} = 0.518 - 0.528 = -0.01$, the effect on $\Delta^{17}O$ is only 1% of the effect on $\delta^{18}O$. Similarly, the fractionation associated with the oxygen isotope exchange between CO_2 and leaf water for $\delta^{18}O$ is $\epsilon^{18}O_{CO2-H2O}$, but the change in $\Delta^{17}O$ is only $(\theta_{H2O-CO2} - \lambda_{RL}) = (0.5229 - 0.528) = -0.0051 \times \epsilon^{18}O_{H2O-CO2}$, thus 0.51% of the change in $\delta^{18}O$ (Hofmann et al. 2017; Koren et al. 2019; Adnew et al. 2020).

Mesophyll conductance calculation

$g_{m\Delta17}$ (mol m^{-2} s^{-1} bar^{-1}) can be derived from measurements of $\Delta^{17}O$ using Equation (6) under the assumptions that (i) the isotopic equilibration between CO_2 and H_2O in the mesophyll is complete ($\theta_{eq} = 1$) and (ii) the oxygen isotopic composition of leaf water at the CO_2–H_2O exchange site is the same as at the evaporation site (Farquhar et al. 1993; Gillon and Yakir 2000a, 2000b; Barbour et al. 2016; Ubierna et al. 2017; Holloway-Phillips et al. 2019).

$$g_{m\Delta17} = \frac{A_n/P}{c_i - c_{m\Delta17}} \quad (6)$$

A_n (μmol m^{-2} s^{-1}) is the assimilation rate, P (bar) is the total atmospheric pressure, c_i (μmol mol^{-1}) is the CO_2 mole fraction in the intercellular air space, and $c_{m\Delta17}$ is the mole fraction at the CO_2–H_2O exchange site, calculated using $\Delta^{17}O$ measurements as follows (see Supplemental data for a detailed derivation):

$$c_{m\Delta17} = c_i\left[\frac{\Delta^{17}O_i - \Delta^{\#17}O_A - \Delta^{*17}O_w}{\Delta^{17}O_m - \Delta^{\#17}O_A - \Delta^{*17}O_w}\right] \quad (7)$$

where $\Delta^{17}O_i$ and $\Delta^{17}O_m$ are the $\Delta^{17}O$ of CO_2 in the intercellular air space and at the CO_2–H_2O exchange site, respectively. $\Delta^{17}O_i$ and $\Delta^{17}O_m$ are calculated from the $\delta^{17}O$ and $\delta^{18}O$ values of CO_2 in the intercellular air space (index i) ($\Delta^{17}O_i = \delta^{17}O_i - \lambda \times \delta^{18}O_i$) and at the CO_2–H_2O exchange site in the mesophyll (index m) ($\Delta^{17}O_m = \delta^{17}O_m - \lambda \times \delta^{18}O_m$). $\Delta^{*17}O_w$ is calculated in a similar manner from the ^{17}O and ^{18}O fractionation of CO_2 during diffusion and dissolution in water (a_{17w} and a_{18w}). $\Delta^{\#17}O_A$ is a modified definition of $\Delta^{17}O$ of the assimilated CO_2 where the individual δ values ($\delta^{17}O_A$ and $\delta^{18}O_A$) are multiplied by α_{17w} and α_{18w}, respectively (Equation (8)).

$$\Delta^{\#\,17}O_A = \delta^{17}O_A \times \alpha_w^{17} - \lambda \times \delta^{18}O_A \times \alpha_w^{18} \quad (8)$$

The analogous equation for the estimate of c_m using $\delta^{18}O$ measurement is shown as Equation (9) (Cernusak et al. 2004; Farquhar and Cernusak 2012; Barbour et al. 2016; Osborn et al. 2017).

$$c_{m18} = c_i\left(\frac{\delta^{18}O_i - \delta^{18}O_A \times \alpha_w^{18} - a_{18w}}{\delta^{18}O_m - \delta^{18}O_A \times \alpha_w^{18} - a_{18w}}\right) \quad (9)$$

The numerical value of a_{18w} is 0.8‰ (Farquhar and Lloyd 1993). The fractionation for $^{12}C^{18}O^{16}O$ during dissolution is −0.8‰ (Vogel et al. 1970).The corresponding fractionation in $^{12}C^{17}O^{16}O$ is −0.418‰, calculated from the $^{12}C^{18}O^{16}O$ fractionation due to equilibrium dissolution using $\theta_{CO2-H2O} = 0.5229$ (Barkan and Luz 2012). We assume that the $^{13}C^{16}O^{16}O$ fractionation during diffusion in water is the same as the fractionation against $^{12}C^{17}O^{16}O$ (Farquhar and Lloyd 1993) and use the average fractionation determined for $^{13}C^{16}O^{16}O$ of 0.8‰ [average of 0.7‰ (O'Leary 1984) and 0.9‰ (Jähne et al. 1987)]. The $^{12}C^{17}O^{16}O$ fractionation due to the sum of the equilibrium dissolution and diffusion in water is then 0.8‰ + (−0.418‰) = 0.382‰ (a_{17w}).

Substituting Equation (7) for $c_{m\Delta17}$ in Equation (6) and rearranging terms, $g_{m\Delta17}$ can be expressed as follows:

$$g_{m\Delta17} = \frac{A_n/P}{c_i - c_{m\Delta17}} = \left(\frac{A_n/P}{c_i}\right)\frac{\Delta^{\#17}O_A + \Delta^{*17}O_w - \Delta^{17}O_m}{\Delta^{17}O_i - \Delta^{17}O_m} \quad (10)$$

In Equation (10), $\Delta^{*17}O_w$ is constant and $\Delta^{17}O_m$ is mainly dependent on the $\Delta^{17}O$ of leaf water. $\Delta^{\#17}O_A$ and $\Delta^{17}O_i$ are dependent on the $\Delta^{17}O$ of the CO_2 entering the cuvette. The θ_{eq} affects $\Delta^{17}O$ of CO_2 at the CO_2–H_2O exchange site, $\Delta^{17}O$ of CO_2 in the intercellular air space, and $\Delta^{17}O$ of the assimilated CO_2. The detailed derivation of Equation (10) is provided in the Supplemental data. The analogous equation for the estimate of g_m using $\delta^{18}O$ measurement is shown as

Equation (11) (Cernusak et al. 2004; Farquhar and Cernusak 2012; Barbour et al. 2016; Osborn et al. 2017):

$$g_{m18} = \frac{A_n/P}{c_i - c_{m18}} = \left(\frac{A_n/P}{c_i}\right) \frac{\delta^{18}O_A \times \alpha_w^{18} + a_{18w} - \delta^{18}O_m}{\delta^{18}O_i - \delta^{18}O_m} \tag{11}$$

The θ_{eq} between CO_2 and H_2O has been the subject of intense discussion. Several studies have indicated that it may not always be unity, especially for plants with lower CA activity and high CO_2 uptake rate (Gillon and Yakir 2000a, 2000b, 2001; Cousins et al. 2006; Studer et al. 2014; Ogée et al. 2018). In vitro CA assay studies using CO_2 concentrations and alkalinity similar to the levels found in leaves suggest that CO_2 should always be in isotope equilibrium with leaf water (Cousins et al. 2007; Studer et al. 2014; Barbour et al. 2016; Ubierna et al. 2017); however, $\Delta_A^{18}O$-drived θ_{eq} values contradict the in vitro CA assays (Cousins et al. 2006). Recently, Ogée et al. (2018) reevaluated published estimates of g_m and θ_{eq}, incorporating the competition between CO_2 hydration and carboxylation and the contribution from respiratory fluxes. They concluded that for C_3 species, θ_{eq} remains close to unity, and for C_4 species (for instance *Zea mays*), θ_{eq} is above 0.75. Furthermore, derived values of g_m and θ_{eq} are not very sensitive to the respiratory fraction for both C_3 and C_4 plants (Ogée et al. 2018). In this study, we investigated the sensitivity of $g_{m\Delta17}$ and g_{m18} estimates to the assumed θ_{eq} ranging from 0.75 to 1 and assuming that the respiratory fractionation is 0.

In addition to estimating mesophyll conductance to the CO_2–H_2O exchange site using the oxygen isotope composition, we calculated g_{m13}, the conductance from the intercellular air space to the chloroplast where the carboxylation takes place using $\delta^{13}C$ of CO_2. A detailed derivation and explanation of g_{m13} is provided in Evans et al. (1986). More information on $\Delta_A^{18}O$ and g_{m18} can be found in Gillon and Yakir (2000a, 2000b), Barbour et al. (2016), and Holloway-Phillips et al. (2019). Supplemental Table S1 in the Supplemental data provides a list of all equations and variables used in this study.

To estimate the precision with which g_{m18} and $g_{m\Delta17}$ can be derived from measurements in gas exchange experiments, we used Monte Carlo simulations of g_m following Holloway-Phillips et al. (2019). Using a leaf cuvette model (Adnew et al. 2020; Koren et al. 2020) and assuming constant assimilation rate, stomatal, and mesophyll conductance, we simulated the mole fraction and isotopic composition of CO_2 in the air surrounding the leaf, in the intercellular air space, and at the CO_2–H_2O exchange site under steady-state conditions, varying the isotopic composition of the incoming CO_2 over a wide range. We then used the model results, including realistic measurement error estimates based on experiments and uncertainties in assumptions, to calculate the apparent discrimination $\Delta_A^{18}O$ and the oxygen isotope composition of the assimilated CO_2 ($\delta^{18}O_A$) (Evans et al. 1986; Barbour et al. 2016) and their uncertainties:

$$\Delta_A^{18}O = \frac{\zeta(\delta^{18}O_a - \delta^{18}O_e)}{1 + \delta^{18}O_a - \zeta(\delta^{18}O_a - \delta^{18}O_e)} \tag{12}$$

$$\delta^{18}O_A = \frac{\delta^{18}O_a - \Delta_A^{18}O}{\Delta_A^{18}O + 1} = \delta^{18}O_a - \zeta(\delta^{18}O_a - \delta^{18}O_e) \tag{13}$$

$\zeta = c_e/(c_e - c_a)$, where c_e and c_a are the mole fraction of CO_2 entering and leaving the cuvette, respectively. $\delta^{18}O_e$ and $\delta^{18}O_a$ are the $\delta^{18}O$ of CO_2 entering and leaving the cuvette, respectively. Details of the model setup are provided in the Supplemental data. Similarly, the photosynthetic discrimination in $\Delta^{17}O$ ($\Delta_A\Delta^{17}O$) is calculated as shown in Equation (14) (Adnew 2020; Adnew et al. 2020).

$$\Delta_A\Delta^{17}O = \frac{\zeta(\Delta^{17}O_a - \Delta^{17}O_e)}{1 + \Delta^{17}O_a - \zeta(\Delta^{17}O_a - \Delta^{17}O_e)} \tag{14}$$

where $\Delta^{17}O_e$ and $\Delta^{17}O_a$ are the $\Delta^{17}O$ of CO_2 entering and leaving the cuvette, respectively.

Results

CO_2 gradient in different leaf compartments and discrimination against ^{18}O and $\Delta^{17}O$ during assimilation

As shown in Table 1 and Fig. 3, the CO_2 mole fraction successively decreases from the cuvette air (set to about 400 μmol mol^{-1} by adjusting the airflow with 500 μmol mol^{-1} of CO_2) to the site of carboxylation during photosynthetic activity. The fast-growing C_3 herbaceous annual sunflower (*Helianthus annuus* L. cv. 'sunny') had a high CO_2 assimilation rate associated with a large conductance for CO_2 diffusion and a high c_m value. This contrasts with the slower growing C_3 evergreen ivy (*Hedera hibernica* L.) that had a much lower assimilation rate, conductance, and c_m. The C_4 herbaceous annual maize (*Z. mays*) combined a high assimilation rate with a low stomatal conductance but a high mesophyll conductance, resulting in a low c_m value. The average fraction of CO_2 entering the leaf that is assimilated, calculated as $(c_a - c_c)/c_a$, is 40% and 50% for sunflower and ivy, respectively (Fig. 3 and Table 1).

Figure 4A shows the discrimination against ^{18}O associated with assimilation ($\Delta_A^{18}O$) for sunflower, ivy, and maize as a function of the c_{m18}/c_a ratio. $\Delta_A^{18}O$ varied with c_{m18}/c_a, in agreement with previous studies (Farquhar et al. 1993; Gillon and Yakir 2000a; Barbour et al. 2016; Osborn et al. 2017). For sunflower, we observe $\Delta_A^{18}O$ values between 29‰ and 64‰ for c_{m18}/c_a between 0.54 and 0.86. Ivy showed relatively little variation of $\Delta_A^{18}O$ around a mean of 22‰ for c_{m18}/c_a between 0.48 and 0.58. For maize, $\Delta_A^{18}O$ and c_{m18}/c_a

Table 1. Summary of gas exchange parameters determined in experiments with sunflower, ivy, and maize

Parameter	Unit	PFD (μmol m^{-2} s^{-1})	Sunflower	Ivy	Maize
A_n	μmol m^{-2} s^{-1}	300	18 (0.7)	12 (0.8)	17 (2)
		1,200	29 (2)	15 (2)	32 (2)
g_s	mol m^{-2} s^{-1}	300	0.49 (0.17)	0.10 (0.02)	0.08 (0.01)
		1,200	0.42 (0.05)	0.15 (0.03)	0.16 (0.02)
g_{m18}	mol m^{-2} s^{-1} bar^{-1}	300	0.53 (0.16)	0.21 (0.05)	0.32 (0.08)
		1,200	0.45 (0.16)	0.18 (0.03)	0.32 (0.02)
$g_{m\Delta17}$	mol m^{-2} s^{-1} bar^{-1}	300 (normal CO_2)	0.57 (single)	0.21 (0.09)	0.36 (0.15)
		300 (^{17}O-enriched CO_2)	0.41 (0.13)	0.14 (0.04)	0.20 (0.07)
		300 (both normal and ^{17}O-enriched CO_2)	0.45 (0.13)	0.17 (0.08)	0.28 (14)
		1,200 (normal CO_2)	0.60 (0.17)	0.17 (0.04)	0.38 (0.23)
		1,200 (^{17}O-enriched CO_2)	0.29 (0.05)	0.15 (0.01)	0.19 (0.03)
		1,200 (both normal and ^{17}O-enriched CO_2)	0.45 (0.21)	0.17 (0.02)	0.31 (0.19)
g_{m13}	mol m^{-2} s^{-1} bar^{-1}	300	0.31 (0.06)	0.18 (0.08)	ND
		1,200	0.29 (0.10)	0.13 (0.02)	ND
c_a	μmol mol^{-1}	All	402 (3)	403 (3)	403 (3)
c_i	μmol mol^{-1}	300	354 (11)	276 (13)	184 (21)
		1,200	321 (10)	295 (13)	184 (16)
c_c	μmol mol^{-1}	300	294 (9)	199 (38)	ND
		1,200	211 (38)	175 (26)	ND
$c_{m\Delta17}$	μmol mol^{-1}	300 (both normal and ^{17}O-enriched CO_2)	300 (6)	207 (36)	120 (41)
		1,200 (both normal and ^{17}O-enriched CO_2)	241 (37)	207 (12)	71 (46)
c_{m18}	μmol mol^{-1}	300	319 (10)	219 (10)	134 (15)
		1,200	256 (26)	213 (12)	89 (17)

The mole fraction of CO_2 at the H_2O–CO_2 exchange site is calculated assuming that the isotopic composition of leaf water at the site of CO_2–H_2O exchange is the same as at the site of evaporation. Numbers in parenthesis are the standard deviation of the mean (1σ). PFD is the photon flux density of photosynthetically active radiation. c_{m18} and $c_{m\Delta17}$ are the mole fraction of CO_2 in the mesophyll calculated from δ^{18}O and Δ^{17}O measurements, respectively.

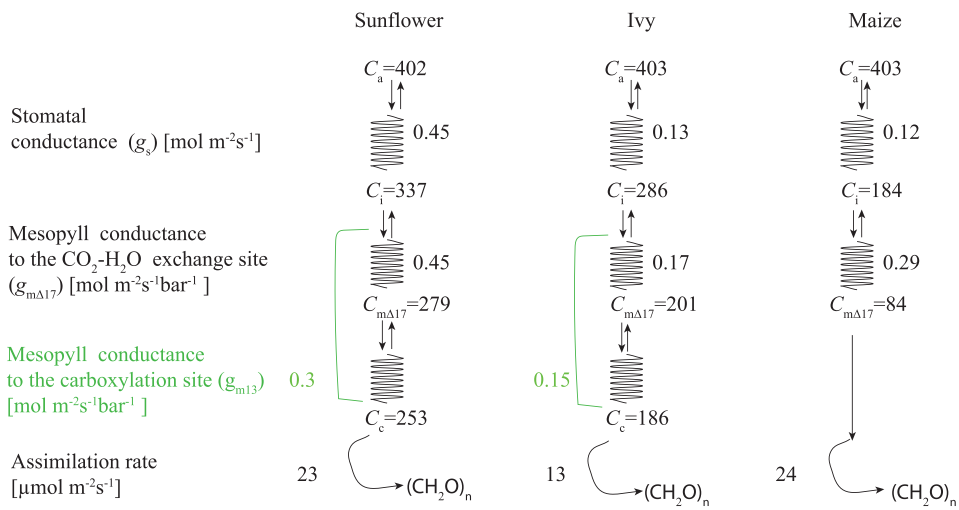

Figure 3. A schematic representation of the various resistances during diffusion of CO_2 in the leaves of two C_3 plants (sunflower and ivy) and one C_4 plant (maize). The data are mean values, where *c* is the mole fraction of CO_2 in μmol mol^{-1} and the subscripts *a*, *i*, *m*, and *c* stand for air surrounding the leaf, intercellular air space, CO_2–H_2O exchange site ("mesophyll"), and chloroplast, respectively. Mean assimilation rates are also indicated.

were lower than for the two C_3 species measured in this study.

Figure 4B shows discrimination against Δ^{17}O associated with assimilation ($\Delta_A\Delta^{17}$O) for sunflower, ivy, and maize as a function of the $c_{m\Delta17}/c_a$ ratio. $\Delta_A\Delta^{17}$O strongly depends on the relative difference in the Δ^{17}O of the CO_2 entering the leaf and Δ^{17}O value of leaf water. When ^{17}O-enriched CO_2 was used (solid symbols), the discrimination against Δ^{17}O was stronger [more negative values, see also Adnew et al. (2020)].

Both Δ_A^{18}O and $\Delta_A\Delta^{17}$O are not intrinsic properties of plant CO_2 uptake, but are strongly dependent on the difference between the oxygen isotope composition of leaf water and of the CO_2 entering the leaf (Cousins et al. 2006; Holloway-Phillips et al. 2019; Adnew et al. 2020). The fractionation associated with the initial fixation by the enzyme

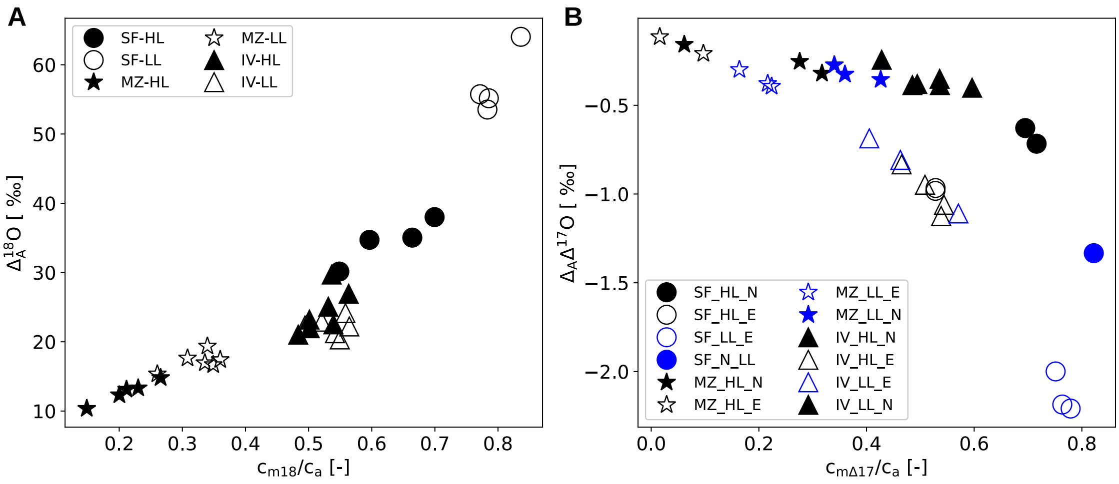

Figure 4. Oxygen isotope discrimination of CO_2 during photosynthetic gas exchange. **A)** Discrimination against ^{18}O ($\Delta_A^{18}O$) during photosynthesis for two C_3 plants, sunflower (SF) and ivy (IV), and the C_4 plant maize (MZ) as a function of c_{m18}/c_a measured in HL and LL conditions. **B)** $\Delta^{17}O$ photosynthetic discrimination ($\Delta_A\Delta^{17}O$) for the same plants as a function of $c_{m\Delta17}/c_a$. N and E stand for normal and ^{17}O-enriched CO_2, respectively. LL and HL stands for low-light and high-light experiments, respectively.

RubiscO (ribulose-1,5-bisphosphate carboxylase-oxygenase) or PEP (phosphoenolpyruvate) has no/negligible effect on the $\delta^{18}O$ and $\Delta^{17}O$ value of CO_2 (Farquhar and Lloyd 1993; Adnew et al. 2021). As a result, $\Delta_A^{18}O$ and $\Delta_A\Delta^{17}O$ can be positive, 0, or negative depending on the oxygen isotope composition of the CO_2 entering the leaf and the isotope composition of leaf water (Adnew 2020). $\Delta_A^{18}O$ is proportional to $c_m/(c_a - c_m) \times (\delta^{18}O_m - \delta^{18}O_a)$ (Farquhar and Lloyd 1993; Hofmann et al. 2017; Koren et al. 2019), and $\Delta_A\Delta^{17}O$ is proportional to $c_m/(c_a - c_m) \times (\Delta^{17}O_m - \Delta^{17}O_a)$ (Hofmann et al. 2017; Koren et al. 2019; Adnew et al. 2020) whereas $\Delta_A^{13}C$ is proportional to $(b - a_{13})c_c/c_a$, where a_{13} is the ^{13}C discrimination due to diffusion and b is the discrimination due to Rubisco (Farquhar et al. 1982, 1989; Farquhar and Lloyd 1993).

Mesophyll conductance

As shown in Fig. 5, the mean $g_{m\Delta17}$ and g_{m18} estimates are similar within the errors for all plant species. Both $g_{m\Delta17}$ and g_{m18} estimates do not show a significant difference when irradiation changes from 300 to 1,200 μmol m^{-2} s^{-1} for all the plant species. As shown in Fig. 5 and Table 1, $g_{m\Delta17}$ estimates for sunflower, ivy, and maize are lower when ^{17}O-enriched CO_2 is used relative to normal CO_2 at all light conditions. The error bars are the standard deviation of the 3 replicates, which include measurement errors and difference between individual leaves. The $g_{m\Delta17}$ and g_{m18} values for the individual experiments are shown Supplemental Fig. S1 of the Supplemental data.

Influence of $\Delta^{17}O_i - \Delta^{17}O_m$ on g_m

Figure 6A shows the error in the $g_{m\Delta17}$ estimates for our experiments as a function of $\Delta^{17}O_i - \Delta^{17}O_m$. As expected, the error in the $g_{m\Delta17}$ estimates is higher at lower $\Delta^{17}O_i - \Delta^{17}O_m$. This can be understood from Equation (10) that is used to calculate $g_{m\Delta17}$: the value of the denominator becomes very small (close to 0) when $\Delta^{17}O$ in the intercellular space and in the mesophyll are very similar, leading to large uncertainties in $g_{m\Delta17}$. To estimate the error in $g_{m\Delta17}$, we assumed a measurement error in $\Delta^{17}O$ of 0.02‰. The $\Delta^{17}O$ errors are much smaller than the error of the individual δ values (Miller et al. 1999). For instance, the typical error for $\delta^{17}O$ and $\delta^{18}O$ of H_2O samples is 0.1‰ to 1‰ whereas the $\Delta^{17}O$ is determined with an error smaller than 0.01‰ (Uemura et al. 2010; Aron et al. 2021). This is partly due to the fact that mass-dependent fractionations during experimental gas handling cancel out (Thiemens 2006). Figure 6B, shows a similar plot for the error in the g_{m18} estimates as a function of $\delta^{18}O_i - \delta^{18}O_m$. Here we assumed an error in $\delta^{18}O$ measurements of 0.6‰ and 0.1‰ for water vapor and CO_2, respectively. Similar to $g_{m\Delta17}$, the error g_{m18} increases when the absolute value of $\delta^{18}O_i - \delta^{18}O_m$ decreases.

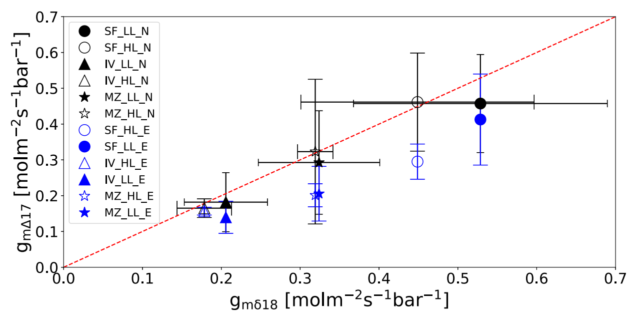

Figure 5. $g_{m\Delta17}$ and g_{m18} estimates for sunflower (SF), ivy (IV), and maize (MZ) at LL (solid) and HL (open). For the $g_{m\Delta17}$ estimate, the experiments were done with enriched CO_2 (E) and with normal CO_2 (N). The error bars represent the standard deviation for replicate experiments ($n = 3$). The dashed line is the 1:1 line.

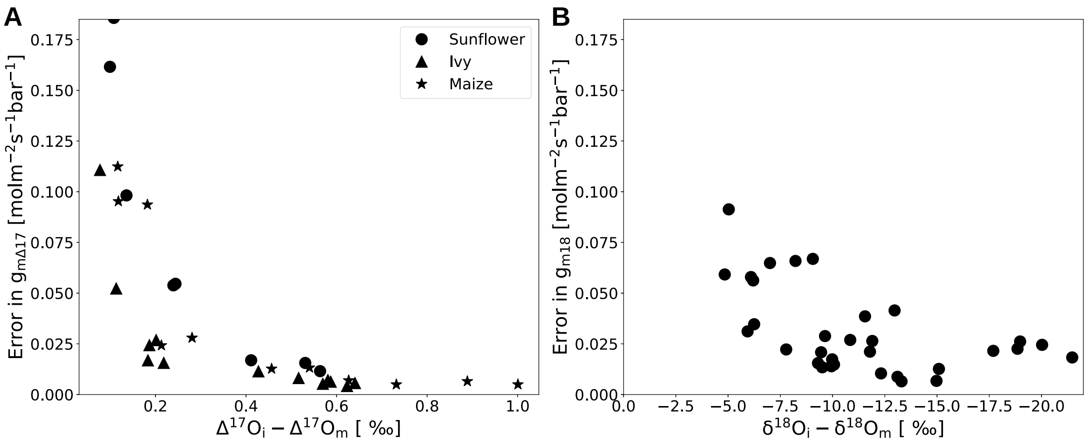

Figure 6. Sensitivity of g_m estimates to the oxygen isotope difference of CO_2 between the intercellular air space and mesophyll. Error in $g_{m\Delta17}$ **A)** and g_{m18} **B)** estimates as a function of $\Delta^{17}O_i - \Delta^{17}O_m$ and $\delta^{18}O_i - \delta^{18}O_m$, respectively. This refers to the overall error of the g_m determination as further explained in the text for the individual experiments.

We evaluated the sensitivity of $g_{m\Delta17}$ to the $\Delta^{17}O$ of CO_2 by investigating ($\Delta^{17}O_i - \Delta^{17}O_m$) differences of 0.2‰, 0.5‰, 1‰, and 1.5‰, respectively, using a leaf cuvette model and Monte Carlo simulations (Fig. 7). The relative error in $g_{m\Delta17}$ due to measurement error increases when the $|\Delta^{17}O_i - \Delta^{17}O_m|$ decreases, as was demonstrated for g_{m18} estimates by Holloway-Phillips et al. (2019). When $|\Delta^{17}O_i - \Delta^{17}O_m|$ is close to 0, the errors in g_m estimates are very large. Also, for $|\Delta^{17}O_i - \Delta^{17}O_m| = 0.5$‰, typical errors are still 50% of the assigned g_m value. Similar Monte Carlo simulations for g_{m18} are shown in the Supplemental data (Supplemental Fig. S2).

Sensitivity of mesophyll conductance to the θ_{eq} and to the choice of the 3-isotope reference slope λ_{RL}

As described in the Introduction, the choice of the reference slope λ_{RL} used for the calculation of $\Delta^{17}O$ values is to a certain degree arbitrary (Hofmann et al. 2012; Adnew et al. 2019). As described above, the precision of $g_{m\Delta17}$ is sensitive to $\Delta^{17}O_i - \Delta^{17}O_m$. We investigated how changes in the assumed θ_{eq} value affect $\Delta^{17}O_i - \Delta^{17}O_m$ and subsequently $g_{m\Delta17}$. Conceptually, we expect that when θ_{eq} is lower, $\Delta^{17}O_m$ is less modified by isotope exchange and thus less different from $\Delta^{17}O_i$. To test the sensitivity of $\Delta^{17}O_i - \Delta^{17}O_m$ on θ_{eq}, we used θ_{eq} ranging from 0.75 to 1 for each experiment to calculate $\Delta^{17}O_m$. Indeed, Supplemental Fig. S3 shows that for each individual experiment, lower values of the assumed θ_{eq} result in a lower $\Delta^{17}O_i - \Delta^{17}O_m$. The effect of θ_{eq} on the $\Delta^{17}O_i - \Delta^{17}O_m$ estimates is linear. Isotope exchange between CO_2 and H_2O in the mesophyll determines both $\Delta^{17}O_m$ and $\delta^{18}O_m$ (Supplemental Fig. S4). $\delta^{18}O_i - \delta^{18}O_m$ also decreases as θ_{eq} decreases from 1 to 0.75 as shown in Supplemental Fig. S3. Figure 8A shows the effect of θ_{eq} on $\Delta^{17}O_i - \Delta^{17}O_m$ (circles) and $\delta^{18}O_i - \delta^{18}O_m$ (stars) for an experiment with $g_{m\Delta17}$ and g_{m18} value of 0.163 mol m^{-2} s^{-1} bar^{-1} and 0.169 mol m^{-2} s^{-1} bar^{-1}, respectively, and $\Delta^{17}O_i - \Delta^{17}O_m$ and $\delta^{18}O_i - \delta^{18}O_m$ differences of 0.486‰ and −9.445‰, respectively, at $\theta_{eq} = 1$. When θ_{eq} decreases, CO_2 equilibrates less with the mesophyll water; thus, $\Delta^{17}O_i - \Delta^{17}O_m$ and $\delta^{18}O_i - \delta^{18}O_m$ decreases ($\Delta^{17}O_m$ and $\delta^{18}O_m$ stay closer to $\Delta^{17}O_i$ and $\delta^{18}O_i$, respectively).

Figure 8B shows the effect of θ_{eq} on the difference $g_{m18} - g_{m\Delta17}$ for the initial conditions mentioned above ($g_{m\Delta17} \cong g_{m18}$). This dependence is a measure of the uncertainty that is introduced to the $g_{m\Delta17}$ and g_{m18} estimates when 100% equilibration is assumed although the equilibration is in fact not complete. When θ_{eq} is lower than 1, g_{m18} and $g_{m\Delta17}$ increase (Supplemental Fig. S5). This is in agreement with the results from Barbour et al. (2016), who showed that the g_{m18} estimates increase when equilibration is assumed to be incomplete. The effect of θ_{eq} on the $g_{m\Delta17}$ and g_{m18} estimates is not linear. An increase in $g_{m18} - g_{m\Delta17}$ with a decrease in θ_{eq} illustrates that g_{m18} estimates are more sensitive to θ_{eq} value compared with $g_{m\Delta17}$ estimates (Supplemental Fig. S5). For further information, the effect of θ_{eq} on $g_{m\Delta17}$ and g_{m18} for all individual experiments is shown in Supplemental Figs. S6 and S7, respectively.

The g_m values also depend on the choice of λ_{RL}. Figure 9 shows the $g_{m\Delta17}$ values and $\Delta^{17}O_i - \Delta^{17}O_m$ determined using λ values between 0.516 and 0.5305. The absolute value of $\Delta^{17}O_i - \Delta^{17}O_m$ is smaller for lower values of λ_{RL} (Fig. 9). The effect of the choice of λ_{RL} is small when the difference $\Delta^{17}O_i - \Delta^{17}O_m$ is high (open symbols); for instance, the $g_{m\Delta17}$ changes only by 0.05 as λ_{RL} changes from 0.516 to 0.5305 for $\Delta^{17}O_i - \Delta^{17}O_m$ of about 0.8‰ as shown in Fig. 9. However, when $\Delta^{17}O_i - \Delta^{17}O_m$ is close to 0 (solid symbols), the choice of λ_{RL} results in a large variation of $g_{m\Delta17}$.

Influence of uncertainty in water isotopic composition on g_m

The oxygen isotope composition of water across a leaf can have a considerable gradient. This causes an uncertainty in

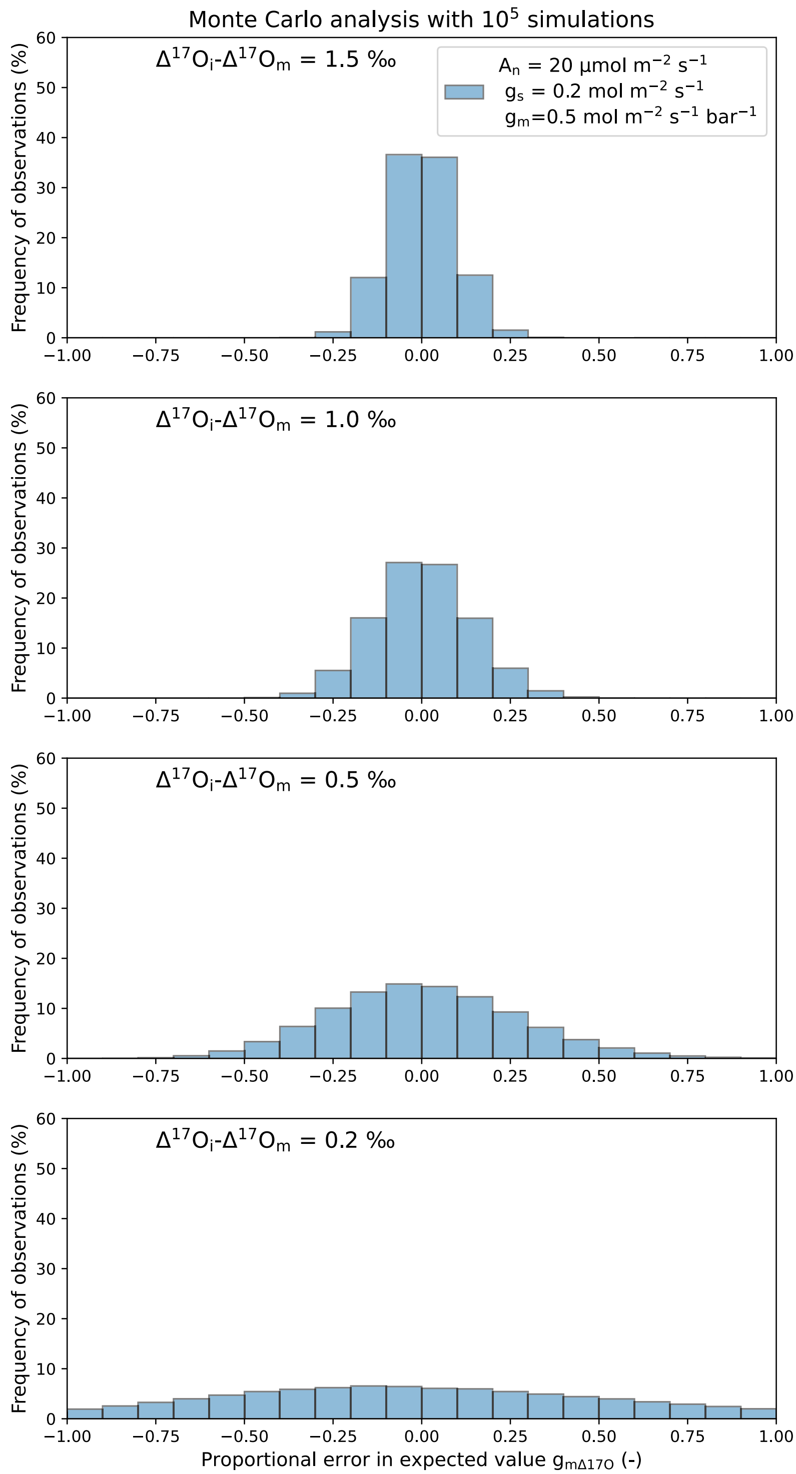

Figure 7. Probability distribution of the error in $g_{m\Delta17}$ [relative error = (simulated $g_{m\Delta17}$ − assigned $g_{m\Delta17}$)/assigned $g_{m\Delta17}$] due to measurement error in the $\Delta^{17}O$ measurements of CO_2 and water vapor for four different values of $\Delta^{17}O_i - \Delta^{17}O_m$, for an "assigned" value of $g_{m\Delta17} = 0.5$ mol m^{-2} s^{-1} bar^{-1}. The analysis is performed with a Monte Carlo approach using simulated gas exchange parameters from the leaf cuvette model. For $\Delta^{17}O$, we assigned an error of 0.01‰, similar to the precision for CO_2 and water vapor $\Delta^{17}O$ measurements. $\Delta^{17}O$ of CO_2 varied from 5‰ to 0‰ to generate the corresponding $\Delta^{17}O_i - \Delta^{17}O_m$ differences. The $\delta^{18}O$ and $\Delta^{17}O$ values of leaf water are 10‰ and 0‰, respectively.

our knowledge of the isotopic composition of water at the site where CO_2–H_2O exchange takes place. This in turn causes an uncertainty in the estimate of the oxygen isotope composition of the CO_2 in equilibrium with the leaf water. Consequently, the oxygen isotope composition of CO_2 in the intercellular air space is not well defined, which affects

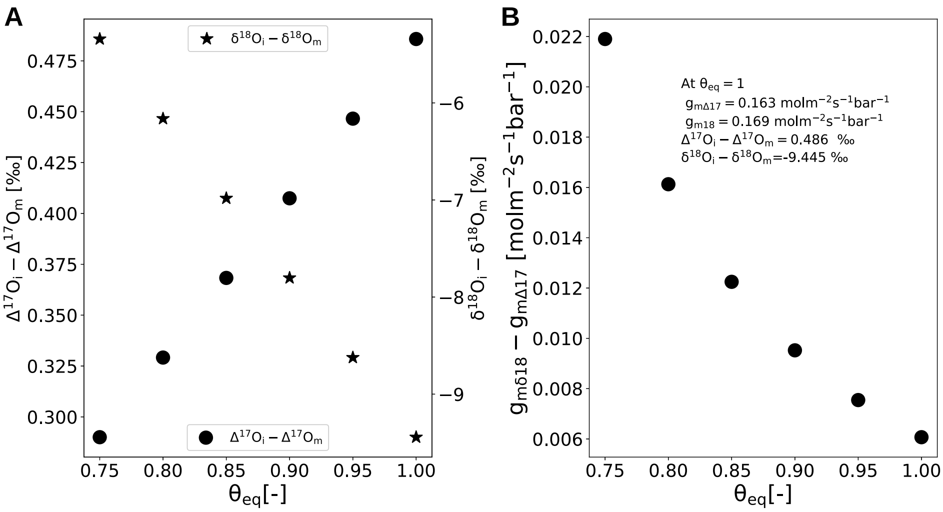

Figure 8. The effect of the assigned θ_{eq} on the CO_2 oxygen isotope composition difference between the intercellular air space and mesophyll. **A)** $\Delta^{17}O_i - \Delta^{17}O_m$ and $\delta^{18}O_i - \delta^{18}O_m$ and **B)** $g_{m18} - g_{m\Delta17}$ values. The g_m values (g_{m18} and $g_{m\Delta17}$) and oxygen isotope differences between the intercellular air space and mesophyll ($\Delta^{17}O$ and $\delta^{18}O$) at $\theta_{eq} = 1$ are determined experimentally. Values at $\theta_{eq} < 1$ are simulated assuming that the other parameters such as the oxygen isotope composition of the CO_2 and water vapor leaving and entering the cuvette, assimilation rate, etc., remain constant.

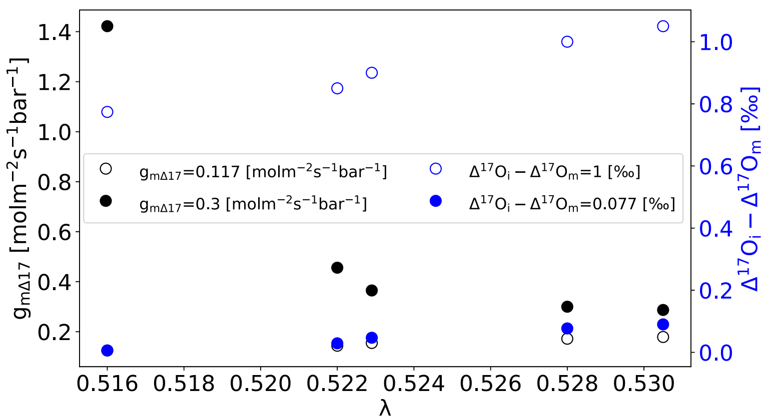

Figure 9. Effect of λ_{RL} on the $g_{m\Delta17}$ estimate. The $g_{m\Delta17}$ and $\Delta^{17}O_i - \Delta^{17}O_m$ values given in the legend are for experiments calculated using $\lambda_{RL} =$ 0.528 (a reference slope used in this study). The $g_{m\Delta17}$ and $\Delta^{17}O_i - \Delta^{17}O_m$ values of the experiments were recalculated using a λ_{RL} ranging from 0.516 to 0.5305.

the g_m estimate [see Equations (10) and (11) for $g_{m\Delta17}$ and g_{m18}, respectively]. We performed a sensitivity analysis to determine the effect of a potential uncertainty in the assumed $\delta^{18}O$ of H_2O at the CO_2–H_2O exchange site in the range of −8‰ to 8‰ on g_{m18} and $g_{m\Delta17}$ estimates. This range is based on published estimates (Gan et al. 2003; Landais et al. 2006; Cernusak et al. 2016). For the comparison, we took the experiment where our g_{m18} and $g_{m\Delta17}$ estimates were similar (0.178 mol m^{-2} s^{-1} bar^{-1} and 0.188 mol m^{-2} s^{-1} bar^{-1}, respectively). The values of $|\Delta^{17}O_i - \Delta^{17}O_m|$ and $|\delta^{18}O_i - \delta^{18}O_m|$ for this experiment were 0.39‰ and 9.4‰, respectively. The corresponding $\delta^{17}O$ value of H_2O is calculated from the $\delta^{18}O$ assuming that the transpired water has a $\Delta^{17}O$ value of typical meteoric water as described in the Materials and methods section ($\Delta^{17}O$ value of CO_2 at the CO_2–H_2O exchange site). As shown in Fig. 10, the induced uncertainty for g_{m18} (Δg_{m18}, stars) is much larger than the one for $g_{m\Delta17}$ ($\Delta g_{m\Delta17}$, circles). This is largely due to the much smaller effect on $|\Delta^{17}O_i - \Delta^{17}O_m|$ compared with $|\delta^{18}O_i - \delta^{18}O_m|$ (color bar).

Discussion

The $g_{m\Delta17}$ values determined from measurements of $\Delta^{17}O$ agree within errors with g_{m18} with an overall *P*-value of 0.876 (for the individual plant species, the *P*-values are 0.598, 0.203, and 0.5475 for sunflower, ivy, and maize, respectively, because they cover smaller ranges). The determination of $g_{m\Delta17}$ using $\Delta^{17}O$ can be improved by measuring $\Delta^{17}O$ of the water vapor leaving and entering the cuvette. This would allow independent assessment of the $\Delta^{17}O$ value of the evaporating water. Measurements of $\Delta^{17}O$ and thus its application to determine $g_{m\Delta17}$ will become technically easier in the future due to laser spectroscopy techniques that enable measurement of the $\Delta^{17}O$ of CO_2 (Steur et al. 2021) and water vapor (Outrequin et al. 2021) with a precision better than 0.01‰.

Our estimates of g_{m18} for sunflower are in good agreement with values reported in previous studies (Shrestha et al. 2019; Adnew et al. 2021). For maize, $g_{m18} = 0.31$ mol m^{-2} s^{-1} bar^{-1} is within the wide range of 0.169 to 0.9 mol m^{-2} s^{-1} bar^{-1} reported in the literature (Flexas et al. 2012; Ubierna et al. 2017, 2018; Kolbe and Cousins 2018; Adnew et al. 2021; Crawford and Cousins 2021). However, Barbour et al. (2016) and Gillon and Yakir (2000a) reported even higher g_{m18} values for maize, 1.78 mol m^{-2} s^{-1} bar^{-1} and 1.0 mol m^{-2} s^{-1} bar^{-1}, respectively. Differences in mesophyll conductance might be caused by different experimental and growing conditions such as temperature, CO_2 mixing ratio, leaf age, and $|\delta^{18}O_i - \delta^{18}O_m|$ (Evans and von Caemmerer 2013; Barbour et al. 2016; Osborn et al. 2017; Ubierna et al. 2017, 2018; Kolbe and Cousins 2018; Holloway-Phillips et al. 2019; Crawford and Cousins 2021). The lower g_m for *Hedera* compared with *Helianthus* might be due to the low mesophyll porosity and thick cell walls of mesophyll cells which hinder the movement of CO_2 within intercellular air space and across cell walls as reported for evergreen woody plants (Niinemets 2016; Veromann-Jürgenson et al. 2017; Carriquí et al. 2020; Eckert et al. 2021; Evans 2021; Flexas et al. 2021). Our results confirm previous findings in C_3 species that g_{m18} is generally higher than g_{m13}, demonstrating that oxygen isotope equilibration between CO_2 and H_2O is achieved in the diffusion pathway before the CO_2 reaches the site of carboxylation for sunflower and ivy (Table 1).

No significant differences in the mesophyll conductance estimates (both $g_{m\Delta17}$ and g_{m18}) were found between PFDs of 300 [low-light (LL)] and 1,200 [high-light (HL)] μmol m^{-2} s^{-1} for the 3 species used in this study. For $g_{m\Delta17}$, the *P*-value between LL and HL experiments is 0.984, 0.786, and 0.652 for sunflower, maize, and ivy, respectively. For g_{m18}, the *P*-value between LL and HL experiments is 0.493, 0.897, and 0.286 for sunflower, maize, and ivy, respectively. This is similar to our earlier results in Adnew et al. (2021), where g_{m18} of sunflower did not show a light intensity effect between 200 and 1,500 μmol m^{-2} s^{-1} and Ogée et al. (2018) where g_{m18} did not show a significant ($P > 0.5$) change with an irradiance change from 150 to 1,500 μmol m^{-2} s^{-1} for *Flaveria bidentis* and tobacco (*Nicotiana tabacum*) leaves.

Estimates of g_m (both $g_{m\Delta17}$ and g_{m18}) increase when we assume a lower θ_{eq}, as reported previously for g_{m18} (Barbour et al. 2016; Ubierna et al. 2017; Ogée et al. 2018). The choice of the three-isotope reference slope does not cause a large uncertainty on $g_{m\Delta17}$ estimates when $|\Delta^{17}O_i - \Delta^{17}O_m|$ is higher than about 0.2‰.

One of the limitations of estimating g_m using the ^{18}O isotope composition is the uncertainty in the $\delta^{18}O$ value of H_2O at the CO_2–H_2O exchange site. Using $\Delta^{17}O$ measurements, the error in the g_m estimate due to the uncertainty in the oxygen isotope composition of leaf water at the CO_2–H_2O exchange site is lower than for the g_{m18} estimate as shown in Fig. 10. The uncertainty introduced in the $\Delta^{17}O$ value of the CO_2 in the mesophyll can be calculated as follows:

$$\begin{aligned}\Delta\Delta^{17}O_m &= (0.5229 - 0.528) \times \Delta\delta^{18}O_{wes} \\ &= 0.0051 \times \Delta\delta^{18}O_{wes}\end{aligned} \quad (15)$$

where 0.5229 is $\theta_{CO2-H2O}$ and 0.528 is the reference slope used in this study. $\Delta\delta^{18}O_{wes}$ is change in the $\delta^{18}O$ of leaf water at the exchange site. $\Delta^{17}O$ changes only by 0.0051‰ for a ‰ change in the $\delta^{18}O$ value leaf water at the CO_2–H_2O exchange site.

Our model calculations highlight a potentially important source of discrepancy of g_m values between different studies, especially when the difference between the isotopic composition of CO_2 in the intercellular air space and the CO_2 in equilibrium with leaf water ($|\delta^{18}O_i - \delta^{18}O_m|$ or $|\Delta^{17}O_i - \Delta^{17}O_m|$) is small. An overestimation of g_m was demonstrated by Holloway-Phillips et al. (2019) for *Vicia faba* when the $\Delta_A^{18}O$ was close to 0. This effect can be compensated to some degree by choosing CO_2 with an oxygen isotopic composition deviating from the CO_2 at the CO_2–H_2O exchange site. The manipulation required in the $\Delta^{17}O$ of the CO_2 to reach a certain precision in $g_{m\Delta17}$ is smaller (in absolute terms) than the manipulation of $\delta^{18}O$ for g_{m18}. The isotopic manipulation can be also done on the $\Delta^{17}O$ and $\delta^{18}O$ values of the water vapor entering the cuvette. We note that there is an important "feedback" between g_m and $|\delta^{18}O_i - \delta^{18}O_m|$ or $|\Delta^{17}O_i - \Delta^{17}O_m|$: when g_m increases, CO_2 exchange between mesophyll and intercellular air space becomes higher, which decreases $|\delta^{18}O_i - \delta^{18}O_m|$ or $|\Delta^{17}O_i - \Delta^{17}O_m|$.

g_m estimates are: (i) strongly dependent on the mole fraction in the intercellular air space (c_i): the lower the c_i, the higher the g_m value is (Osborn et al. 2017; Ubierna et al. 2017, 2018; Kolbe and Cousins 2018; Crawford and Cousins 2021), and (ii) strongly dependent on the $|\Delta^{17}O_i - \Delta^{17}O_m|$ and $|\delta^{18}O_i - \delta^{18}O_m|$ (Figs. 6 and 7). We recommended reporting the oxygen isotope difference between the intercellular air space and mesophyll and the mole fraction of CO_2 in the intercellular air space along with other parameters for better comparison between the g_m estimates from different studies.

Conclusion

The feasibility of using $\Delta^{17}O$ to estimate g_m in a gas exchange experiment from $\Delta^{17}O$ measurements of the CO_2 and H_2O entering and leaving a leaf cuvette is demonstrated in this study. Based on the model developed by Farquhar and Cernusak (2012) for $\delta^{18}O$, we derived the mathematical formalism for calculating $g_{m\Delta17}$ from $\Delta^{17}O$ of CO_2 and leaf water during a gas exchange experiment. An important parameter in the determination of g_m by oxygen isotopes is the difference between the oxygen isotopic composition of CO_2 in the intercellular air space and at the CO_2–H_2O exchange site. The uncertainty in the $g_{m\Delta17}$ estimates due to a potentially erroneous estimate of θ_{eq} is lower compared with the g_{m18} estimate for consistent differences $|\Delta^{17}O_i - \Delta^{17}O_m|$ and $|\delta^{18}O_i - \delta^{18}O_m|$. The choice of the three-isotope exponent (λ) is not a limiting factor for using $\Delta^{17}O$ measurements as a tracer for mesophyll conductance if $|\Delta^{17}O_i - \Delta^{17}O_m|$ is not close to 0. The sensitivity of both oxygen isotope techniques can be enhanced by using H_2O and/or CO_2 with large differences in $\delta^{18}O$ and $\Delta^{17}O$ between the intercellular air space and the CO_2–H_2O exchange site, by modifying the isotopic composition of the CO_2. Nevertheless, the oxygen isotope techniques are prone to larger errors for plant species with high mesophyll conductance where $|\Delta^{17}O_i - \Delta^{17}O_m|$ and $|\delta^{18}O_i - \delta^{18}O_m|$ will be smaller regardless of the $\Delta^{17}O$ and $\delta^{18}O$ value of the CO_2 entering the cuvette.

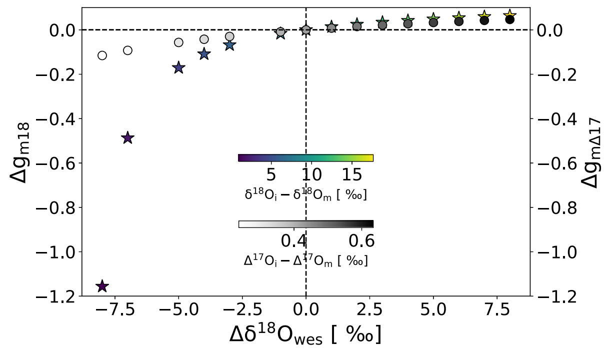

Figure 10. Uncertainty in g_{m18} (stars) and $g_{m\Delta17}$ (circle) estimates when the CO_2–H_2O exchange happens at a different isotope compositions than assumed (or calculated for the evaporation site). The difference in g_m is the difference in g_m between the assigned value and g_m calculated at a different value of $\delta^{18}O_{wes}$. The different g_{m18} and $g_{m\Delta17}$ values are simulated assuming all the other parameters such as the oxygen isotope composition of the CO_2 and water vapor leaving and entering the cuvette, assimilation rate, etc., remain constant. The color bars are different for $\Delta^{17}O_i - \Delta^{17}O_m$ and $\delta^{18}O_i - \delta^{18}O_m$.

Materials and methods

Plant material and growth conditions

Plant growth and experimental conditions have been described in detail in Adnew et al. (2020) and are briefly summarized here. Plants were grown in a controlled environment growth room at air temperature 20 °C, relative humidity 70%, PFD 300 μmol m^{-2} s^{-1}, and a photoperiod of 16 h. A dwarf variety of sunflower (*H. annuus* L. cv. 'sunny'), an herbaceous C_3 species with the highest c_m/c_a ratio (Adnew et al. 2021), was grown from seed in 0.6-L pots. The first leaf pair was used for the experiments, which reached the final size after about 4 week of growth. Later appearing leaves above were removed to avoid shading of the target leaves. For ivy (*H. hibernica* L.), a woody C_3 species with an intermediate c_m/c_a ratio, established juvenile plants were used. They were grown in 6-L pots and pruned when placed in the growth room. Leaves that had developed to maturity in the growth room were used for the experiments. Maize (*Z. mays* L. cv. 'saccharate'), an herbaceous C_4 species with the lowest c_m/c_a ratio, was grown from seed in 1.6-L pots. After at least 7 week, the 4th or higher leaf number was used for the experiments when fully grown. A section of the leaf at about 1/3 from the tip was used for the experiments.

Gas exchange experiments

Gas exchange experiments were performed in a flow-through system with a leaf cuvette that had a window of 7 × 7 cm. A detailed description of the leaf cuvette is provided in Pons and Welschen (2002) and Adnew et al. (2021). The air temperature was kept at 20 ° C using a temperature-controlled water bath (Tamson TLC 3, The Netherlands). Leaf temperature was measured with a K type thermocouple. A fan inside mixed the air thoroughly and kept boundary layer conductance high, about 5 mol m^{-2} s^{-1}depending on leaf size, as determined according to Parkinson (1985). Experiments were performed at two PFDs, the growth PFD of 300 μmol m^{-2} s^{-1} (LL) and a higher PFD closer to light saturation of 1,200 μmol m^{-2} s^{-1} (HL). For each experiment, a single leaf was used. For each experimental condition, replicate measurements were carried out. All the data are evaluated using python, and the *P*-value is calculated using the "Scipy.stats.ttest_ind" python package. The *P*-value is determined by comparing the *t*-statistic of the observed data against a theoretical *t*-distribution.

Compressed outside air was passed through soda lime to scrub the CO_2, and pure CO_2 was injected to produce a CO_2 mole fraction of 500 μmol mol^{-1} with well-known isotopic composition. Airflow through the cuvette with the leaf was adjusted to result in a mole fraction in outgoing air of 400 μmol mol^{-1}. The large drawdown of 100 μmol mol^{-1} was necessary to produce a sufficiently large isotope signal. The air was humidified and kept at a specified dew point by leading it through a temperature-controlled column. The humidity of the air entering the cuvette was adjusted based on H_2O partial pressure of the air leaving the cuvette to avoid condensation which was monitored with a dew point meter (HYGRO-M1, General Eastern, Watertown, MA, USA). The CO_2 mole fraction of air entering and leaving the cuvette was measured with an infrared gas analyzer in absolute mode (IRGA, model LI-6262, LI-COR Inc., NE, USA). The mole fraction and isotopic composition of water vapor were measured with a water vapor isotope analyzer (WVIA, model 911-0034, Los Gatos Research, USA). The mole fraction of CO_2, and the mole fraction and isotope composition of water vapor of the air entering the cuvette were measured for about 10 min, whereas the air

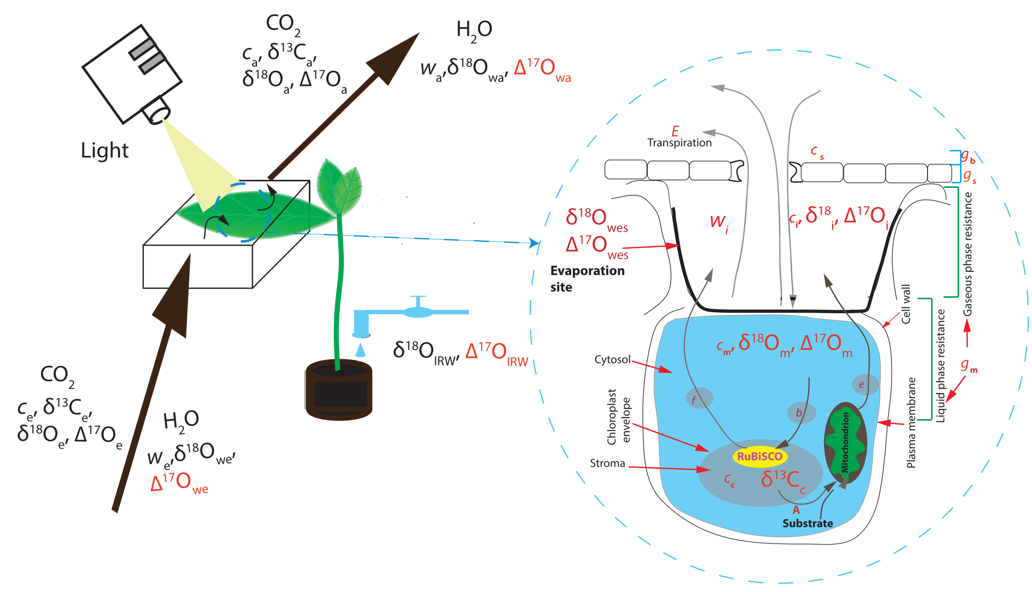

Figure 11. Schematic of the gas exchange experiment. Parameters in black are measured and parameters in red are calculated or assumed. IRW refers to irrigation water. *c* and *w* stand for mole fraction of CO_2 and water, respectively, and the subscripts *e*, *a*, *s*, *i*, *es*, *m*, and *c* stand for entering the cuvette, leaving the cuvette, leaf surface, intercellular air space, mesophyll, evaporation site, and chloroplast, respectively. g_b, g_s, and g_m stand for boundary layer conductance, stomatal conductance, and mesophyll conductance, respectively.

leaving the cuvette was measured until steady state was reached (about 2 h). Figure 11 shows a simplified schematic for the experimental setup showing the parameters measured and assumed or calculated during this study.

Two types of CO_2 were used, "normal" CO_2 (Air Products, Germany) and ^{17}O-enriched CO_2. The latter was prepared by photochemical isotope exchange between CO_2 and O_2 induced by a UV lamp (Shaheen et al. 2007; Adnew et al. 2019). The $\delta^{18}O$ of the CO_2 entering the cuvette ranged from 27.25‰ to 30.49‰. The $\delta^{13}C$ of the CO_2 ranged from −10.23‰ to −3.27‰. The $\delta^{13}C$ and $\delta^{18}O$ values were determined by measuring the CO_2 against a working standard on an isotope ratio mass spectrometer (IRMS) in a dual-inlet mode where the working standards were calibrated against NBS 19. For "normal CO_2," $\Delta^{17}O_e = -0.333$‰ for all experiments and plant types. Enriched CO_2 had $\Delta^{17}O_e = 0.22$‰ for the experiments with sunflower and maize and $\Delta^{17}O_e = 0.34$‰ for ivy.

Measurements started after the experimental conditions in the leaf exchange system had reached steady state in terms of the rates of CO_2 uptake and transpiration, and the δD and $\delta^{18}O$ of water vapor leaving the cuvette. Gas exchange variables were recorded, and subsequently, the air was collected in 3 2-L glass flasks after passing through a $Mg(ClO_4)_2$ dryer. Leaf area was measured with a LI-3100C area meter (Li-COR, Inc., USA). After the experiment, the leaf was placed in a closed glass vial and kept in a freezer at −20 °C until leaf water extraction. Leaf water was extracted by cryogenic vacuum distillation for 4 h at 60 °C following a well-established procedure (Landais et al. 2006). The $\delta^{17}O$ and $\delta^{18}O$ of leaf water were determined at the Laboratoire des Sciences du Climat et de l'Environnement using a fluorination technique.

Carbon dioxide extraction and isotope analysis

CO_2 was extracted from the air samples cryogenically in a system made from electropolished stainless steel. Our system used 4 commercial traps (MassTech, Bremen, Germany). The first 2 traps were operated at dry ice temperature (−78 °C) to remove moisture and some organics. The other 2 traps were operated at liquid nitrogen temperature (−196 ° C) to trap CO_2. The extracted CO_2 was first measured for $\delta^{13}C$ and $\delta^{18}O$ with a $Delta^{Plus}XL$ IRMS (Thermo Fisher, Germany) in dual-inlet mode. After the isotope measurement, the remaining gas in the bellow of the IRMS was frozen back into the break seal tube for the measurement of $\Delta^{17}O$. The $\Delta^{17}O$ of CO_2 was determined using the CO_2–O_2 exchange method (Barkan et al. 2015; Adnew et al. 2019). A detailed description of the CO_2–O_2 exchange system at Utrecht University is given in Adnew et al. (2019, 2022). Equal amounts of CO_2 and O_2 were mixed in a quartz reactor containing a platinum sponge catalyst at the bottom and heated at 750 °C for 2 h. After isotope equilibration, the CO_2 was trapped at liquid nitrogen temperature, while the O_2 was collected with 1 pellet of 5 Å molecular sieve (1.6 mm, Sigma-Aldrich, USA) at liquid nitrogen temperature. The isotopic composition of the isotopically equilibrated O_2 was measured with a $Delta^{Plus}XL$ IRMS in dual-inlet mode with reference to a pure O_2 working gas that has been assigned values of $\delta^{17}O = 9.254$‰ and $\delta^{18}O = 18.542$‰ by measurements of multiple aliquots by E. Barkan at the Hebrew University of Jerusalem.

Monte Carlo simulation and leaf cuvette model

In our leaf cuvette model, the leaf is partitioned into 3 different reservoirs: the intercellular air space, the mesophyll cell, and the chloroplast (Adnew et al. 2020; Koren et al. 2020). For this model, we assumed an infinite boundary layer conductance. In the leaf model, we used a 100 μmol mol^{-1} drawdown of CO_2 similar to the photosynthesis experiments. The assimilation rate was set to 20.0 μmol m^{-2} s^{-1}, and the leaf area and flow rate of air were set to 30 cm^2 and 0.7 L min^{-1}, respectively. For the purpose of simulation, we used the bulk leaf water measurements as the reference value for the evaporative site H_2O isotope composition. These values were 5.39‰ and 10.648‰ in δ^{17}O and δ^{18}O, respectively, which was the mean of the δ^{17}O and δ^{18}O values of bulk leaf water measured for sunflower, ivy, and maize in our experiments. The δ^{18}O of the CO_2 entering the cuvette was 30.47‰, which is the δ^{18}O value of the CO_2 used in the experiments (normal CO_2 experiments). The leaf cuvette model has been explained in detail in Adnew et al. (2020), and the model code is available at https://git.wur.nl/leaf_model/D17O (Koren et al. 2020).

To investigate the dependency of g_m estimates on the measurement error at different values of $\Delta^{17}O_i - \Delta^{17}O_m$, we first calculated an isotopic steady state (i.e. mole fractions and δ values in each of the compartments) for a leaf cuvette experiment using the leaf cuvette model described above. Δ^{17}O of CO_2 entering the cuvette ($\Delta^{17}O_e$) was set to values between 0‰ and 4.8‰, which resulted in $\Delta^{17}O_i - \Delta^{17}O_m$ differences of 0.2‰ to 1.5‰, respectively (Fig. 10), to evaluate the sensitivity of $g_{m\Delta17}$ on the measurement error depending on $\Delta^{17}O_i - \Delta^{17}O_m$ differences. The δ^{18}O value of the CO_2 entering the cuvette was varied between 30.47‰ and 53.4‰.

Δ^{17}O value of CO_2 at the CO_2–H_2O exchange site

In this study, we did not measure the δ^{17}O value of the water vapor entering and leaving the cuvette. The δ^{17}O value of the water at the evaporation site was calculated based on the assumption that the isotopic composition of transpired water was the same as the source water (steady state) (Harwood et al. 1998; Yepez et al. 2007; Welp et al. 2008; Cernusak et al. 2016) and the source water had a similar Δ^{17}O value as meteoric water (Hofmann et al. 2017; Koren et al. 2019; Adnew et al. 2020). The δ^{17}O of the transpired water was calculated from the δ^{18}O value of the transpired water and the Δ^{17}O value of the meteoric water (Luz and Barkan 2010) as follows:

$$\delta^{17}O_{trans} = \exp^{(0.033+0.528\times\log(\delta^{18}O_{trans}+1))} - 1 \quad (16)$$

where $\delta^{18}O_{trans}$ is δ^{18}O value of the transpired water and calculated as follows:

$$\delta^{18}O_{trans} = \left(\frac{w_a}{w_a - w_e}\right) \times (\delta^{18}O_{wa} - \delta^{18}O_{we}) + \delta^{18}O_{we} \quad (17)$$

w_e and w_a are the mole fractions of water entering and leaving the cuvette, respectively, and $\delta^{18}O_{we}$ and $\delta^{18}O_{wa}$ are the corresponding δ^{18}O values. The δ^{17}O value of water at the evaporation site ($\delta^{17}O_{wes}$) is then calculated from the $\delta^{17}O_{trans}$, $\delta^{18}O_{trans}$ and δ^{18}O of water at the evaporation site ($\delta^{18}O_{wes}$) as follows:

$$\delta^{17}O_{wes} = \left(\frac{\delta^{18}O_{wes}+1}{\delta^{18}O_{trans}+1}\right)^{\lambda_{trans}} \times (\delta^{17}O_{trans}+1) - 1 \quad (18)$$

where λ_{trans} is the three-isotope exponent for transpiration (Landais et al. 2006) which depends on humidity of air (RH) and is calculated as

$$\lambda_{trans} = 0.522 - 0.008 \times \text{RH for } 0.3 \leq \text{RH} \leq 1 \quad (19)$$

$\delta^{18}O_{wes}$ is calculated as follows:

$$\delta^{18}O_{wes} = (1+\varepsilon^{18}_{equ})\left[(1+\varepsilon^{18}_{k})(1+\delta^{18}O_{wa})\left(1-\frac{w_a}{w_i \times h}\right) + \frac{w_a}{w_i \times h}(1+{}^{18}O_{trans})\right] - 1 \quad (20)$$

where ϵ^{18}_{equ} is the equilibrium fractionation between liquid water and vapor, and ϵ^{18}_{k} is the fractionation of water vapor as it diffuses through stomata and leaf boundary layer. w_i is the mole fraction of water vapor in the intercellular air space, and h is the humidity in the intercellular air space.

The ^{17}O isotopic composition of CO_2 at the CO_2–H_2O exchange site ($\delta^{17}O_m$) is calculated as follows:

$$\delta^{17}O_m = \theta_{equ} \times \left(\left(\frac{\delta^{18}O_m+1}{\delta^{18}O_{wes}+1}\right)^{0.5229} \times (\delta^{17}O_{wes}+1) - 1\right) + (1-\theta_{equ}) \times \delta^{17}O_{mo} \quad (21)$$

where 0.5229 is the three-isotope exponent for the CO_2–H_2O isotope exchange (Barkan and Luz 2012). In case of incomplete equilibration, the fraction of ^{17}O isotopic composition CO_2 in the mesophyll that has not equilibrated with mesophyll water, $\delta^{17}O_{mo}$, is calculated as follows (Cernusak et al. 2004; Farquhar and Cernusak 2012):

$$\delta^{17}O_{mo} = \delta^{17}O_a - \bar{a}_{17}\left(1-\frac{c_c}{c_a}\right) \quad (22)$$

where $\bar{a}_{17}$ is the diffusional fractionation of ^{17}O of CO_2 that can be calculated as follows (Farquhar and Lloyd 1993; Cernusak et al. 2004; Farquhar and Cernusak 2012):

$$\bar{a}_{17} = \frac{(c_i - c_{m17})a_{17w} + (c_s - c_i)a_{17s} + (c_a - c_s)a_{17b}}{c_a - c_{m17}} \quad (23)$$

$\delta^{18}O_m$ is the $\delta^{18}O$ of CO_2 at the CO_2–H_2O exchange site (in the mesophyll), calculated as follows:

$$\delta^{18}O_m = \delta^{18}O_{wes} \times \theta_{equ} \times (1 + \varepsilon_w^{18}) + \theta_{equ} \times \varepsilon_w^{18} + (1 - \theta_{equ}) \times \delta^{18}O_{mo} \quad (24)$$

where ϵ_w^{18} is ^{18}O isotope fractionation during the CO_2–H_2O isotope exchange (Brenninkmeijer et al. 1983):

$$\varepsilon_w = \frac{17{,}604}{T_{leaf}} - 17.93 \quad (25)$$

$\delta^{18}O_{mo}$ is the isotope composition of CO_2 in the mesophyll that has not equilibrated with mesophyll water which is calculated as follows (Cernusak et al. 2004; Farquhar and Cernusak 2012):

$$\delta^{18}O_{mo} = \delta^{18}O_a - \bar{a}_{18}\left(1 - \frac{c_c}{c_a}\right) \quad (26)$$

where $\bar{a}_{18}$ is the diffusional fractionation of ^{18}O of CO_2 that can be calculated as follows (Farquhar and Lloyd 1993; Cernusak et al. 2004; Farquhar and Cernusak 2012):

$$\bar{a}_{18} = \frac{(c_i - c_{m18})a_{18w} + (c_s - c_i)a_{18s} + (c_a - c_s)a_{18b}}{c_a - c_{m18}} \quad (27)$$

Finally, the $\Delta^{17}O$ value of CO_2 at the exchange site ($\Delta^{17}O_m$) is calculated as follows:

$$\Delta^{17}O_m = \delta^{17}O_m - 0.528 \times \delta^{18}O_m \quad (28)$$

Alternative equations for calculating $\Delta^{17}O_m$ ($\Delta^{17}O$ value of CO_2 at the exchange site) are shown from Equations (29) to (31). The $\Delta^{17}O$ value of CO_2 in equilibrium with the leaf water ($\Delta^{17}O_{mequ}$) can be calculated from the $\Delta^{17}O$ value of leaf water and the equilibrium fractionation between water and CO_2 as follows:

$$\Delta^{17}O_{mequ} = \Delta^{17}O_{wes} + (0.5229 - 0.528) \times \varepsilon_{H_2O\text{-}CO_2} \quad (29)$$

The $\Delta^{17}O$ value of CO_2 in equilibrium value of CO_2 in the mesophyll which is not equilibrated with leaf water ($\Delta^{17}O_{mo}$) can be calculated as follows:

$$\Delta^{17}O_{mo} = \Delta^{17}O_a - (\bar{a}_{17} - 0.528 \times \bar{a}_{18}) \times \left(1 - \frac{c_c}{c_a}\right) \quad (30)$$

Equation (28) can be expressed using Equations (23) and (24) as follows:

$$\Delta^{17}O_m = \theta_{equ} \times \Delta^{17}O_{meq} + (1 - \theta_{equ}) \times \Delta^{17}O_{mo} \quad (31)$$

Acknowledgments

The authors thank Leonard I. Wassenaar and Stefan Terzer-Wassmuth from the International Atomic and Energy Agency, Vienna, for supplying water standards. The authors thank Eugeni Barkan and Rolf Vieten from the Hebrew University of Jerusalem for calibration of our O_2 and CO_2 working gases. We are grateful to Amaelle Landais from the Laboratoire des Sciences du Climat et de l'Environnement at Université Paris-Saclay for measuring the $\Delta^{17}O$ of leaf water samples for our study. We appreciate the helpful suggestions provided by the editor Graham D. Farquhar, reviewer Meisha Holloway-Phillips and three anonymous reviewers, which improved the accessibility of the manuscript for a broader audience.

Author contributions

G.A.A. and T.R. designed the experimental setup for measurement of $\Delta^{17}O$ of CO_2. G.A.A., T.P., and T.L.R. designed the leaf gas exchange measurements. G.A.A. and T.L.P. performed the leaf cuvette experiment and sampling. G.A.A. performed all measurements and data analysis. G.K. provided the leaf cuvette model, Monte Carlo simulation, and interpretation of the results. All authors contributed to the scientific interpretation. G.A.A. and T.R. wrote the manuscript with input from all authors.

Supplemental data

The following materials are available in the online version of this article.

Supplemental Materials and Methods. Equations used to calculate g_{m13}, g_{m18}, and $g_{m\Delta17}$. For $g_{m\Delta17}$, the detailed derivation is provided.

Supplemental Figure S1. $g_{m\Delta17}$ as a function of $\Delta^{17}O_i - \Delta^{17}O_m$ and g_{m18} as a function of $\delta^{18}O_i - \delta^{18}O_m$ for the individual measurements.

Supplemental Figure S2. Probability distribution of the error in g_{m18} [relative error = (simulated g_{m18} − assigned g_{m18})/assigned g_{m18}] due to measurement error in the $\delta^{18}O$ measurements of CO_2 and water vapor for 4 different values of $\delta^{18}O_i$-$\delta^{18}O_m$, for an "assigned" value of g_{m18} = 0.5 mol m^{-2} s^{-1} bar^{-1}.

Supplemental Figure S3. The dependency between of $\Delta^{17}O_i - \Delta^{17}O_m$ and $\delta^{18}O_i - \delta^{18}O_m$ for different values of θ_{eq} (color code).

Supplemental Figure S4. Dependency of the $\Delta^{17}O$ and $\delta^{18}O$ values of CO_2 at the CO_2–H_2O exchange site on the θ_{eq} between the CO_2 and H_2O for the experiments presented in this paper.

Supplemental Figure S5. The sensitivity of derived g_{m18} and $g_{m\Delta17}$ values in our experiments on the assumed value of θ_{eq}.

Supplemental Figure S6. The sensitivity of derived $g_{m\Delta17}$ values in our experiments on the assumed value of θ_{eq}. The color indicates the value of $\Delta^{17}O_i - \Delta^{17}O_m$.

Supplemental Figure S7. The sensitivity of derived g_{m18} values in our experiments on the assumed value of θ_{eq}. The color indicates $\delta^{18}O_i - \delta^{18}O_m$.

Supplemental Table S1. List of variables and equations used in this study to calculate gas exchange parameters and carbon and oxygen 3-isotope discriminations.

Funding

This work was funded by the EU ERC project ASICA. G.A.A. and G.K. received funding from ERC under the ASICA project (ID: 649087).

Conflict of interest statement. None declared.

Data availability

All the data used in this study are provided in the form of figure and tables.

References

Adnew GA. The effect of photosynthetic gas exchange on $\Delta^{17}O$ of atmospheric CO_2 [PhD thesis]; 2020. p. 1–174.

Adnew GA, Hofmann MEG, Paul D, Laskar A, Surma J, Albrecht N, Pack A, Schwieters J, Koren G, Peters W, et al. Determination of the triple oxygen and carbon isotopic composition of CO_2 from atomic ion fragments formed in the ion source of the 253 ultra high-resolution isotope ratio mass spectrometer. Rapid Commun Mass Spectrom. 2019:**33**(17):1363–1380. https://doi.org/10.1002/rcm.8478

Adnew GA, Hofmann MEG, Pons TL, Koren G, Ziegler M, Lourens LJ, Röckmann T. Leaf scale quantification of the effect of photosynthetic gas exchange on Δ_{47} of CO_2. Sci Rep. 2021:**11**(1):14023. https://doi.org/10.1038/s41598-021-93092-0

Adnew GA, Pons TL, Koren G, Peters W, Röckmann T. Leaf-scale quantification of the effect of photosynthetic gas exchange on $\Delta^{17}O$ of atmospheric CO_2. Biogeosciences. 2020:**17**(14):3903–3922. https://doi.org/10.5194/bg-17-3903-2020

Adnew GA, Workman E, Janssen C, Röckmann T. Temperature dependence of isotopic fractionation in the CO_2-O_2 isotope exchange reaction. Rapid Commun Mass Spectrom. 2022:**36**(12):e9301. https://doi.org/10.1002/rcm.9301

Angert A, Rachmilevitch S, Barkan E, Luz B. Effects of photorespiration, the cytochrome pathway, and the alternative pathway on the triple isotopic composition of atmospheric O_2. Glob Biogeochem Cycles. 2003:**17**(1):1030. https://doi.org/10.1029/2002GB001933

Aron PG, Levin NE, Beverly E, Huth TE, Passey BH, Pelletier EM, Poulsen CJ, Winkelstern IZ, Yarian DA. Triple oxygen isotopes in the water cycle. Chem Geol. 2021:**565**:120026. https://doi.org/10.1016/j.chemgeo.2020.120026

Badger MR, Price GD. The role of carbonic anhydrase in photosynthesis. Annu Rev Plant Biol. 1994:**45**(1):369–392. https://doi.org/10.1146/annurev.pp.45.060194.002101

Barbour MM, Evans JR, Simonin KA, von Caemmerer S. Online CO_2 and H_2O oxygen isotope fractionation allows estimation of mesophyll conductance in C_4 plants, and reveals that mesophyll conductance decreases as leaves age in both C_4 and C_3 plants. New Phytol. 2016:**210**(3):875–889. https://doi.org/10.1111/nph.13830

Barkan E, Luz B. High precision measurements of $^{17}O/^{16}O$ and $^{18}O/^{16}O$ ratios in H_2O. Rapid Commun Mass Spectrom. 2005:**19**(24):3737–3742. https://doi.org/10.1002/rcm.2250

Barkan E, Luz B. Diffusivity fractionations of $H_2^{16}O/H_2^{17}O$ and $H_2^{16}O/H_2^{18}O$ in air and their implications for isotope hydrology. Rapid Commun Mass Spectrom. 2007:**21**(18):2999–3005.

Barkan E, Luz B. High-precision measurements of $^{17}O/^{16}O$ and $^{18}O/^{16}O$ ratios in CO_2. Rapid Commun Mass Spectrom. 2012:**26**(23):2733–2738. https://doi.org/10.1002/rcm.6400

Barkan E, Musan I, Luz B. High-precision measurements of $\delta^{17}O$ and ^{17}O-excess of NBS19 and NBS18. Rapid Commun Mass Spectrom. 2015:**29**(23):2219–2224. https://doi.org/10.1002/rcm.7378

Brenninkmeijer CAM, Kraft P, Mook WG. Oxygen isotope fractionation between CO_2 and H_2O. Chem Geol. 1983:**41**:181–190. https://doi.org/10.1016/S0009-2541(83)80015-1

Cao X, Liu Y. Equilibrium mass-dependent fractionation relationships for triple oxygen isotopes. Geochim Cosmochim Acta. 2011:**75**(23):7435–7445. https://doi.org/10.1016/j.gca.2011.09.048

Carriquí M, Nadal M, Clemente-Moreno MJ, Gago J, Miedes E, Flexas J. Cell wall composition strongly influences mesophyll conductance in gymnosperms. Plant J. 2020:**103**(4):1372–1385. https://doi.org/10.1111/tpj.14806

Cernusak LA, Barbour MM, Arndt SK, Cheesman AK, English NB, Feild TS, Helliker BR, Holloway-Phillips MM, Holtum JA, Kahmen A, et al. Stable isotopes in leaf water of terrestrial plants. Plant Cell Environ. 2016:**39**(5):1087–1102. https://doi.org/10.1111/pce.12703

Cernusak LA, Farquhar GD, Wong SC, Stuart-Williams H. Measurement and interpretation of the oxygen isotope composition of carbon dioxide respired by leaves in the dark. Plant Physiol. 2004:**136**(2):3350–3363. https://doi.org/10.1104/pp.104.040758

Cousins AB, Badger MR, von Caemmerer S. A transgenic approach to understanding the influence of carbonic anhydrase on $C^{18}OO$ discrimination during C_4 photosynthesis. Plant Physiol. 2006:**142**(2):662–672. https://doi.org/10.1104/pp.106.085167

Cousins AB, Baroli I, Badger MR, Ivakov A, Lea PJ, Leegood RC, von Caemmerer S. The role of phosphoenolpyruvate carboxylase during C_4 photosynthetic isotope exchange and stomatal conductance. Plant Physiol. 2007:**145**(3):1006–1017. https://doi.org/10.1104/pp.107.103390

Cousins AB, Mullendore DL, Sonawane BV. Recent developments in mesophyll conductance in C_3, C_4 and CAM plants. Plant J. 2020:**101**(4):816–830. https://doi.org/10.1111/tpj.14664

Crawford JD, Cousins AB. Limitation of C_4 photosynthesis by low CA activity increases with temperature but does not influence mesophyll CO_2 conductance. J Exp Bot. 2021:**73**(3):927–938. https://doi.org/10.1093/jxb/erab464

DiMario RJ, Quebedeaux JC, Longstreth DJ, Dassanayake M, Hartman MM, Moroney JV. The cytoplasmic carbonic anhydrases βCA_2 and βCA_4 are required for optimal plant growth at low CO_2. Plant Physiol. 2016:**171**(1):280–293. https://doi.org/10.1104/pp.15.01990

Eckert D, Martens HJ, Gu L, Jensen AM. CO_2 refixation is higher in leaves of woody species with high mesophyll and stomatal resistances to CO_2 diffusion. Tree Physiol. 2021:**41**(8):1450–1461. https://doi.org/10.1093/treephys/tpab016

Evans JR. Mesophyll conductance: walls, membranes and spatial complexity. New Phytol. 2021:**229**(4):1864–1876. https://doi.org/10.1111/nph.16968

Evans JR, Kaldenhoff R, Genty B, Terashima I. Resistances along the CO_2 diffusion pathway inside leaves. J Exp Bot. 2009:**60**(8):2235–2248. https://doi.org/10.1093/jxb/erp117

Evans JR, Sharkey TD, Berry JA, Farquhar GD. Carbon isotope discrimination measured concurrently with gas exchange to investigate CO_2 diffusion in leaves of higher plants. Funct Plant Biol. 1986:**13**(2):281–292. https://doi.org/10.1071/PP9860281

Evans JR, von Caemmerer S. Temperature response of carbon isotope discrimination and mesophyll conductance in tobacco. Plant Cell

Environ. 2013:**36**(4):745–756. https://doi.org/10.1111/j.1365-3040.2012.02591.x

Fabre N, Reiter IM, Becuwe-Linka N, Genty B, Rumeau D. Characterization and expression analysis of genes encoding alpha and beta carbonic anhydrases in Arabidopsis. Plant Cell Environ. 2007:**30**(5):617–629. https://doi.org/10.1111/j.1365-3040.2007.01651.x

Farquhar GD, Cernusak LA. Ternary effects on the gas exchange of isotopologues of carbon dioxide. Plant Cell Environ. 2012:**35**(7):1221–1231. https://doi.org/10.1111/j.1365-3040.2012.02484.x

Farquhar GD, Cernusak LA, Barnes B. Heavy water fractionation during transpiration. Plant Physiol. 2007:**143**(1):11–18. https://doi.org/10.1104/pp.106.093278

Farquhar GD, Ehleringer JR, Hubick KT. Carbon isotope discrimination and photosynthesis. Annu Rev Plant Physiol Plant Mol Biol. 1989:**40**(1):503–537. https://doi.org/10.1146/annurev.pp.40.060189.002443

Farquhar GD, Lloyd J. Carbon and oxygen isotope effects in the exchange of carbon dioxide between terrestrial plants and the atmosphere. London: Acadamic Press Inc; 1993.

Farquhar GD, Lloyd J, Taylor JA, Flanagan LB, Syvertsen JP, Hubick KT, Wong SC, Ehleringer JR. Vegetation effects on the isotope composition of oxygen in atmospheric CO_2. Nature. 1993:**363**(6428):439–443. https://doi.org/10.1038/363439a0

Farquhar GD, O'Leary MH, Berry JA. On the relationship between carbon isotope discrimination and the intercellular carbon dioxide concentration in leaves. Funct Plant Biol. 1982:**9**(2):121–137. https://doi.org/10.1071/PP9820121

Flexas J, Barbour MM, Brendel O, Cabrera HM, Carriquí M, Díaz-Espejo A, Douthe C, Dreyer E, Ferrio JP, Gago J, et al. Mesophyll diffusion conductance to CO_2: an unappreciated central player in photosynthesis. Plant Sci. 2012:**193–194**:70–84. https://doi.org/10.1016/j.plantsci.2012.05.009

Flexas J, Clemente-Moreno MJ, Bota J, Brodribb TJ, Gago J, Mizokami Y, Nadal M, Perera-Castro AV, Roig-Oliver M, Sugiura D, et al. Cell wall thickness and composition are involved in photosynthetic limitation. J Exp Bot. 2021:**72**(11):3971–3986. https://doi.org/10.1093/jxb/erab144

Flexas J, Diaz-Espejo A, Galmes J, Kaldenhoff R, Medrano H, Ribas-Carbo M. Rapid variations of mesophyll conductance in response to changes in CO_2 concentration around leaves. Plant Cell Environ. 2007:**30**(10):1284–1298. https://doi.org/10.1111/j.1365-3040.2007.01700.x

Flexas J, Niinemets U, Gallé A, Barbour MM, Centritto M, Diaz-Espejo A, Douthe C, Galmés J, Ribas-Carbo M, Rodriguez PL, et al. Diffusional conductances to CO_2 as a target for increasing photosynthesis and photosynthetic water-use efficiency. Photosynth Res. 2013:**117**(1–3):45–59. https://doi.org/10.1007/s11120-013-9844-z

Gan KS, Wong SC, Yong JWH, Farquhar GD. ^{18}O spatial patterns of vein xylem water, leaf water, and dry matter in cotton leaves. Plant Physiol. 2002:**130**(2):1008–1021. https://doi.org/10.1104/pp.007419

Gan KS, Wong SC, Yong JWH, Farquhar GD. Evaluation of models of leaf water ^{18}O enrichment using measurements of spatial patterns of vein xylem water, leaf water and dry matter in maize leaves. Plant Cell Environ. 2003:**26**(9):1479–1495. https://doi.org/10.1046/j.1365-3040.2003.01070.x

Gat JR. Oxygen and hydrogen isotopes in the hydrologic cycle. Annu Rev Earth Planet Sci. 1996:**24**(1):225–262. https://doi.org/10.1146/annurev.earth.24.1.225

Gillon JS, Yakir D. Internal conductance to CO_2 diffusion and $C^{18}OO$ discrimination in C_3 leaves. Plant Physiol. 2000a:**123**(1):201–214. https://doi.org/10.1104/pp.123.1.201

Gillon JS, Yakir D. Naturally low carbonic anhydrase activity in C_4 and C_3 plants limits discrimination against $C^{18}OO$ during photosynthesis. Plant Cell Environ. 2000b:**23**(9):903–915. https://doi.org/10.1046/j.1365-3040.2000.00597.x

Gillon J, Yakir D. Influence of carbonic anhydrase activity in terrestrial vegetation on the ^{18}O content of atmospheric CO_2. Science. 2001:**291**(5513):2584–2587. https://doi.org/10.1126/science.1056374

Gonfiantini R, Wassenaar LI, Araguas-Araguas L, Aggarwal PK. A unified Craig-Gordon isotope model of stable hydrogen and oxygen isotope fractionation during fresh or saltwater evaporation. Geochim Cosmochim Acta. 2018:**235**:224–236. https://doi.org/10.1016/j.gca.2018.05.020

Harwood KG, Gillon JS, Griffiths H, Broadmeadow MSJ. Diurnal variation of $\Delta^{13}CO_2$, $\Delta C^{18}O^{16}O$ and evaporative site enrichment of $\delta H_2^{18}O$ in Piper aduncum under field conditions in Trinidad. Plant Cell Environ. 1998:**21**(3):269–283. https://doi.org/10.1046/j.1365-3040.1998.00276.x

Hayles JA, Cao X, Bao H. The statistical mechanical basis of the triple isotope fractionation relationship. Geochem Perspect Lett. 2017:**3**(1):1–11. https://doi.org/10.7185/geochemlet.1701

Hayles JA, Killingsworth BA. Constraints on triple oxygen isotope kinetics. Chem Geol. 2022:**589**:120646. https://doi.org/10.1016/j.chemgeo.2021.120646

Helliker BR, Ehleringer JR. Establishing a grassland signature in veins: ^{18}O in the leaf water of C_3 and C_4 grasses. Proc Natl Acad Sci U S A. 2000:**97**(14):7894–7898. https://doi.org/10.1073/pnas.97.14.7894

Hoag KJ, Still CJ, Fung IY, Boering KA. Triple oxygen isotope composition of tropospheric carbon dioxide as a tracer of terrestrial gross carbon fluxes. Geophys Res Lett. 2005:**32**(2):L02802. https://doi.org/10.1029/2004GL021011

Hofmann MEG, Horváth B, Pack A. Triple oxygen isotope equilibrium fractionation between carbon dioxide and water. Earth Planet Sci Lett. 2012:**319**:159–164. https://doi.org/10.1016/j.epsl.2011.12.026

Hofmann MEG, Horváth B, Schneider L, Peters W, Schützenmeister K, Pack A. Atmospheric measurements of $\Delta^{17}O$ in CO_2 in Göttingen, Germany reveal a seasonal cycle driven by biospheric uptake. Geochim Cosmochim Acta. 2017:**199**:143–163. https://doi.org/10.1016/j.gca.2016.11.019

Holloway-Phillips M, Cernusak LA, Stuart-Williams H, Ubierna N, Farquhar GD. Two-source $\delta^{18}O$ method to validate the $CO^{18}O$-photosynthetic discrimination model: implications for mesophyll conductance. Plant Physiol. 2019:**181**(3):1175–1190. https://doi.org/10.1104/pp.19.00633

Jähne B, Münnich KO, Bösinger R, Dutzi A, Huber W, Libner P. On the parameters influencing air-water gas exchange. J Geophys Res Oceans. 1987:**92**(C2):1937–1949. https://doi.org/10.1029/JC092iC02p01937

Knauer J, Zaehle S, Kauwe MGD, Bahar NH, Evans JR, Medlyn BE, Reichstein M, Werner C. Effects of mesophyll conductance on vegetation responses to elevated CO_2 concentrations in a land surface model. Glob Change Biol. 2019:**25**(5):1820–1838. https://doi.org/10.1111/gcb.14604

Kolbe AR, Cousins AB. Mesophyll conductance in Zea mays responds transiently to CO_2 availability: implications for transpiration efficiency in C_4 crops. New Phytol. 2018:**217**(4):1463–1474. https://doi.org/10.1111/nph.14942

Koren G, Adnew GA, Röckmann T, Peters W. Leaf conductance model for $\Delta^{17}O$ in CO_2; 2020. https://git.wur.nl/leaf_model.

Koren G, Schneider L, van der Velde IR, van Schaik E, Gromov SS, Adnew GA, Mrozek Martino DJ, Hofmann ME, Liang MC, Mahata S, et al. Global 3-D simulations of the triple oxygen isotope signature $\Delta^{17}O$ in atmospheric CO_2. J Geophys Res Atmos. 2019:**124**(15):8808–8836. https://doi.org/10.1029/2019JD030387

Landais A, Barkan E, Luz B. Record of $\delta^{18}O$ and ^{17}O-excess in ice from Vostok Antarctica during the last 150,000 years. Geophys Res Lett. 2008:**35**(2):L02709. https://doi.org/10.1029/2007GL032096

Landais A, Barkan E, Yakir D, Luz B. The triple isotopic composition of oxygen in leaf water. Geochim Cosmochim Acta. 2006:**70**(16): 4105–4115. https://doi.org/10.1016/j.gca.2006.06.1545

Liang M-C, Mahata S, Laskar AH, Thiemens MH, Newman S. Oxygen isotope anomaly in tropospheric CO_2 and implications for CO_2 residence time in the atmosphere and gross primary productivity. Sci Rep. 2017:**7**(1):13180. https://doi.org/10.1038/s41598-017-12774-w

Luz B, Barkan E. Variations of $^{17}O/^{16}O$ and $^{18}O/^{16}O$ in meteoric waters. Geochim Cosmochim Acta. 2010:**74**(22):6276–6286. https://doi.org/10.1016/j.gca.2010.08.016

Mahata S, Bhattacharya SK, Wang C-H, Liang M-C. Oxygen isotope exchange between O_2 and CO_2 over hot platinum: an innovative technique for measuring $\Delta^{17}O$ in CO_2. Anal Chem. 2013:**85**(14): 6894–6901. https://doi.org/10.1021/ac4011777

Matsuhisa Y, Goldsmith JR, Clayton RN. Mechanisms of hydrothermal crystallization of quartz at 250 °C and 15 kbar. Geochim Cosmochim Acta. 1978:**42**(2):173–182. https://doi.org/10.1016/0016-7037(78)90130-8

McManus JB, Nelson DD, Shorter JH, Jimenez R, Herndon S, Saleska S, Zahniser M. A high precision pulsed quantum cascade laser spectrometer for measurements of stable isotopes of carbon dioxide. J Mod Optic. 2005:**52**(16):2309–2321. https://doi.org/10.1080/09500340500303710

Meijer H, Li W. The use of electrolysis for accurate ^{17}O and ^{18}O isotope measurements in water isotopes. Isotopes Environ Health Stud. 1998:**34**(4):349–369. https://doi.org/10.1080/10256019808234072

Miller MF, Franchi IA, Sexton AS, Pillinger CT. High precision $\delta^{17}O$ isotope measurements of oxygen from silicates and other oxides: method and applications. Rapid Commun Mass Spectrom. 1999:**13**-(13):1211–1217. https://doi.org/10.1002/(SICI)1097-0231(19990715)13:13<1211::AID-RCM576>3.0.CO;2-M

Niinemets Ü. Does the touch of cold make evergreen leaves tougher? Tree Physiol. 2016:**36**(3):267–272. https://doi.org/10.1093/treephys/tpw007

Ogée J, Wingate L, Genty B. Estimating mesophyll conductance from measurements of $C^{18}OO$ photosynthetic discrimination and carbonic anhydrase activity. Plant Physiol. 2018:**178**(2):728–752. https://doi.org/10.1104/pp.17.01031

O'Leary MH. Measurement of the isotope fractionation associated with diffusion of carbon dioxide in aqueous solution. J Phys Chem. 1984:**88**(4):823–825. https://doi.org/10.1021/j150648a041

Osborn HL, Alonso-Cantabrana H, Sharwood RE, Covshoff S, Evans JR, Furbank RT, von Caemmerer S. Effects of reduced carbonic anhydrase activity on CO_2 assimilation rates in *Setaria viridis*: a transgenic analysis. J Exp Bot. 2017:**68**(2):299–310. https://doi.org/10.1093/jxb/erw357

Outrequin C, Alexandre A, Vallet-Coulomb C, Piel C, Devidal S, Landais A, Couapel M, Mazur J-C, Peugeot C, Pierre M, et al. The triple oxygen isotope composition of phytoliths, a new proxy of atmospheric relative humidity: controls of soil water isotope composition, temperature, CO_2 concentration and relative humidity. Clim Past. 2021:**17**(5):1881–1902. https://doi.org/10.5194/cp-17-1881-2021

Parkinson KJ. A simple method for determining the boundary layer resistance in leaf cuvettes. Plant Cell Environ. 1985:**8**(3):223–226. https://doi.org/10.1111/1365-3040.ep11604618

Peters W, van der Velde IR, Van Schaik E, Miller JB, Ciais P, Duarte HF, van der Laan-Luijkx IT, van der Molen MK, Scholze M, Schaefer K, et al. Increased water-use efficiency and reduced CO_2 uptake by plants during droughts at a continental scale. Nat Geosci. 2018:**11**(10):744–748. https://doi.org/10.1038/s41561-018-0212-7

Pons TL, Flexas J, von Caemmerer S, Evans JR, Genty B, Ribas-Carbo M, Brugnoli E. Estimating mesophyll conductance to CO_2: methodology, potential errors, and recommendations. J Exp Bot. 2009:**60**(8):2217–2234. https://doi.org/10.1093/jxb/erp081

Pons TL, Welschen RAM. Overestimation of respiration rates in commercially available clamp-on leaf chambers. Complications with measurement of net photosynthesis. Plant Cell Environ. 2002:**25**-(10):1367–1372. https://doi.org/10.1046/j.1365-3040.2002.00911.x

Risi C, Landais A, Winkler R, Vimeux F. Can we determine what controls the spatio-temporal distribution of d-excess and ^{17}O-excess in precipitation using the LMDZ general circulation model? Clim Past. 2013:**9**(5):2173–2193. https://doi.org/10.5194/cp-9-2173-2013

Shaheen R, Janssen C, Röckmann T. Investigations of the photochemical isotope equilibrium between O_2, CO_2 and O_3. Atmos Chem Phys. 2007:**7**(2):495–509. https://doi.org/10.5194/acp-7-495-2007

Shrestha A, Song X, Barbour MM. The temperature response of mesophyll conductance, and its component conductances, varies between species and genotypes. Photosynth Res. 2019:**141**(1):65–82. https://doi.org/10.1007/s11120-019-00622-z

Song X, Simonin KA, Loucos KE, Barbour MM. Modelling non-steady-state isotope enrichment of leaf water in a gas-exchange cuvette environment. Plant Cell Environ. 2015:**38**(12):2618–2628. https://doi.org/10.1111/pce.12571

Steur PM, Scheeren HA, Nelson DD, McManus JB, Meijer HAJ. Simultaneous measurement of $\delta^{13}C$, $\delta^{18}O$ and $\delta^{17}O$ of atmospheric CO_2—performance assessment of a dual-laser absorption spectrometer. Atmos Meas Tech. 2021:**14**(6):4279–4304. https://doi.org/10.5194/amt-14-4279-2021

Stoltmann T, Casado M, Daeron M, Landais A, Kassi S. Direct, precise measurements of isotopologue abundance ratios in CO_2 using molecular absorption spectroscopy: application to $\Delta^{17}O$. Anal Chem. 2017:**89**(19):10129–10132. https://doi.org/10.1021/acs.analchem.7b02853

Studer AJ, Gandin A, Kolbe AR, Wang L, Cousins AB, Brutnell TP. A limited role for carbonic anhydrase in C_4 photosynthesis as revealed by a ca1ca2 double mutant in maize. Plant Physiol. 2014:**165**(2): 608–617. https://doi.org/10.1104/pp.114.237602

Thiemens MH. History and applications of mass-independent isotope effects. Annu Rev Earth Planet Sci. 2006:**34**(1):217–262. https://doi.org/10.1146/annurev.earth.34.031405.125026

Thiemens MH, Chakraborty S, Jackson TL. Decadal $\Delta^{17}O$ record of tropospheric CO_2: verification of a stratospheric component in the troposphere. J Geophys Res Atmos. 2014:**119**(10):6221–6229. https://doi.org/10.1002/2013JD020317

Tholen D, Ethier G, Genty B, Pepin S, Xin-Guang Z. Variable mesophyll conductance revisited: theoretical background and experimental implications. Plant Cell Environ. 2012:**35**(12):2087–2103. https://doi.org/10.1111/j.1365-3040.2012.02538.x

Tomás M, Flexas J, Copolovici L, Galmés J, Hallik L, Medrano H, Ribas-Carbó M, Tosens T, Vislap V, Niinemets Ü. Importance of leaf anatomy in determining mesophyll diffusion conductance to CO_2 across species: quantitative limitations and scaling up by models. J Exp Bot. 2013:**64**(8):2269–2281. https://doi.org/10.1093/jxb/ert086

Ubierna N, Gandin A, Boyd RA, Cousins AB. Temperature response of mesophyll conductance in three C_4 species calculated with two methods: ^{18}O discrimination and in vitro Vpmax. New Phytol. 2017:**214**(1):66–80. https://doi.org/10.1111/nph.14359

Ubierna N, Gandin A, Cousins AB. The response of mesophyll conductance to short-term variation in CO_2 in the C_4 plants *Setaria viridis* and Zea mays. J Exp Bot. 2018:**69**(5):1159–1170. https://doi.org/10.1093/jxb/erx464

Uemura R, Barkan E, Abe O, Luz B. Triple isotope composition of oxygen in atmospheric water vapor. Geophys Res Lett. 2010:**37**(4): L04402. https://doi.org/10.1029/2009GL041960

Veromann-Jürgenson L-L, Tosens T, Laanisto L, Niinemets Ü. Extremely thick cell walls and low mesophyll conductance: welcome to the world of ancient living!. J Exp Bot. 2017:**68**(7):1639–1653. https://doi.org/10.1093/jxb/erx045

Vogel JC, Grootes PM, Mook WG. Isotopic fractionation between gaseous and dissolved carbon dioxide. Zeitschrift für Physik A Hadrons and nuclei. 1970:**230**(3):225–238. https://doi.org/10.1007/BF01394688

Von Caemmerer S, Farquhar GD. Some relationships between the biochemistry of photosynthesis and the gas exchange of leaves. Planta. 1981:**153**(4):376–387. https://doi.org/10.1007/BF00384257

Von Caemmerer S, Ghannoum O, Pengelly JJL, Cousins AB. Carbon isotope discrimination as a tool to explore C_4 photosynthesis. J Exp Bot. 2014:**65**(13):3459–3470. https://doi.org/10.1093/jxb/eru127

Warren C. Estimating the internal conductance to CO_2 movement. Funct Plant Biol. 2006:**33**(5):431–442. https://doi.org/10.1071/FP05298

Welp LR, Lee X, Kim K, Griffis TJ, Billmark KA, Baker JM. $\Delta^{18}o$ of water vapour, evapotranspiration and the sites of leaf water evaporation in a soybean canopy. Plant Cell Environ. 2008:**31**(9):1214–1228. https://doi.org/10.1111/j.1365-3040.2008.01826.x

Yepez EA, Scott RL, Cable WL, Williams DG. Intraseasonal variation in water and carbon dioxide flux components in a semiarid riparian woodland. Ecosystems. 2007:**10**:1100–1115. https://doi.org/10.1007/s10021-007-9079-y

Young ED, Galy A, Nagahara H. Kinetic and equilibrium mass-dependent isotope fractionation laws in nature and their geochemical and cosmochemical significance. Geochim Cosmochim Acta. 2002:**66**(6):1095–1104. https://doi.org/10.1016/S0016-7037(01)00832-8